NBSIR 81-2337

Measurement and Evaluation Methods for an Angular Accelerometer

U.S. DEPARTMENT OF COMMERCE
National Bureau of Standards
National Engineering Laboratory
Center for Electronics and Electrical Engineering
Electrosystems Division
Washington, DC 20234

January 1981

Final Report

Issued August 1981

Under Department of Transportation Reimbursable Agreement
DOT-HS-0-02193IA

Prepared for:
Department of Transportation
national Highway Traffic Safety Administration
400 Seventh St., S.W.
Washington, DC 20590

NBSIR 81-2337

MEASUREMENT AND EVALUATION METHODS FOR AN ANGULAR ACCELEROMETER

John D. Ramboz

U.S. DEPARTMENT OF COMMERCE
National Bureau of Standards
National Engineering Laboratory
Center for Electronics and Electrical Engineering
Electrosystems Division
Washington, DC 20234

January 1981

Final Report

Issued August 1981

Under Department of Transportation Reimbursable Agreement
DOT-HS-9-02193IA

Prepared for:
Department of Transportation
National Highway Traffic Safety Administration
400 Seventh St., S.W.
Washington, DC 20590

U.S. DEPARTMENT OF COMMERCE, Malcolm Baldrige, *Secretary*
NATIONAL BUREAU OF STANDARDS, Ernest Ambler, *Director*

Foreword

Work described herein was performed for the National Highway Traffic Safety Administration (NHTSA) of the Department of Transportation (DoT) under an Interagency Reimbursable Agreement DoT-HS-9-02193IA. The NBS Cost Center for this project was 7223403. Laboratory efforts commenced on October 1, 1980 and were completed on December 30, 1980. The DoT/NHTSA Technical Contract Monitor was Mr. Mark Haffner.

The tests performed and discussed in this report are abbreviated measurements to assess the principal operating characteristics of a newly developed angular accelerometer. Time and funding constraints required that only selected fundamental measurements could be made. As a result of these measurements, satisfactory performance was indicated and further consideration should be given to additional work for the development and testing of this type of transducer. Because of the limited testing, this conclusion is preliminary. Further testing should be done in order to reach final conclusions as to the overall performance for the intended DoT application.

Certain commercial equipment, instruments, or materials are identified in this report in order to adequately specify the experimental procedure. In no case does such identification imply recommendation or endorsement by the National Bureau of Standards, nor does it imply that the material or equipment identified is necessarily the best available for the purpose.

TABLE OF CONTENTS

TABLE OF CONTENTS (cont.)

TABLE OF CONTENTS (cont.)

MEASUREMENT AND EVALUATION METHODS FOR AN ANGULAR ACCELEROMETER

John D. Ramboz

A transducer which measures angular acceleration along one axis was investigated to assess three of its performance characteristics, viz., sensitivity factor, amplitude linearity, and response to linear (non-angular) input accelerations. Accelerometer specifications and response theory are presented. Test philosophy and methodology are discussed along with measurement results. Tests were conducted over a frequency range from 1.5 to 100 Hz and over an acceleration range from 64 to 5000 rad/s^2. Generally, the performance observed was in agreement with the manufacturer's preliminary specifications.

Key words: angular acceleration; angular accelerometer; calibration; instrumentation; measurement; shock and vibration.

1. INTRODUCTION

The Department of Transportation, National Highway Traffic Safety Administration (DoT/NHTSA), Biomechanics Branch is studying the mechanisms of human head impact injury and is developing injury tolerance criteria. An understanding of these mechanisms and use of the tolerance criteria will be of immediate benefit to automotive occupant protection and protection headgear design. These are intended to contribute to the established national goal of improved highway safety.

The measurement of angular head motions during impact has posed a serious challenge to available instrumentation. To date, this difficult measurement has not been successfully performed without large errors and ambiguities. Measurement methods in the past have relied on either photographic techniques or the derivation of angular motions from linear motion measurements. Neither technique has proven totally satisfactory and is, in any instance, very laborious.

In an attempt to establish head injury criteria, a program which employs athletic boxers is being pursued by the DoT. Head motions will be measured and analyzed along with qualified biomedical

observations. Correlation between the measured data and apparent "injury" will lead to a threshold criteria useful in automobile occupant safety.

Transducer attachment to the boxer's head will be made by incorporating the instrumentation, including a multichannel FM transmitter, in the orthodontic mouthpiece. Thus, with the mouthpiece tightly gripped between the teeth, three-dimensional head motion can be sensed and data transmitted to a ringside receiver and recorder. This approach is feasible only if a suitably small and accurate transducer is available to sense the head motions.

A newly developed transducer [1][1] which senses angular acceleration is being investigated for possible use in the "mouthpiece." Its small size, ruggedness, and frequency response make it attractive to consider for this application. A preliminary set of measurements was desired to ascertain the fundamental operating characteristics of this transducer. Based on the preliminary findings, a decision can then be made as to whether to invest additional resources for an in-depth evaluation of such an accelerometer.

The tests performed and discussed herein are designed to determine the angular-acceleration sensitivity factor (i.e., transfer function), the frequency response, amplitude linearity, transverse sensitivity, and linear acceleration sensitivity. These were felt to be the most important of the parameters and could be assessed with hardware and methods already available. Programmatic constraints on time and funds necessitated a brief, but meaningful, set of tests. These are described in this report. However, to characterize fully the transducer's performance, additional tests would be required, but were not performed at this time.

2. ACCELEROMETER SPECIFICATIONS AND PHYSICAL DESCRIPTION

The angular accelerometer available for testing was a developmental prototype and, as such, may not have had all the engineering refinements incorporated into its design. However, it was deemed worthwhile to test it at this stage of its development in order to determine its feasibility for use in the DoT "mouthpiece" configuration.

The manufacturer's preliminary specifications which accompanied the accelerometer are reproduced in appendix A. The parameters of key interest in this phase of the investigation are listed as follows:

---

[1]Numbers in brackets refer to the references listed at the end of this report.

1. Sensitivity,
2. Frequency response,
3. Amplitude linearity,
4. Transverse-axis angular sensitivity, and
5. Linear acceleration sensitivity.

Each of these parameters is briefly discussed and interpreted.

2.1 Angular Acceleration Sensitivity

The sensitivity factor for the transducer is the mechanical-to-electrical transfer function. As such, the transfer function is a complex ratio of the electrical output divided by the mechanical input. The electrical output is voltage and the mechanical input is angular acceleration in units of radians per unit time squared, or rad/s^2. The accelerometer transduction element contains an electrical four-arm Wheatstone bridge where all four arms are active strain sensing elements. The sensitivity factor is, therefore, a function of the bridge excitation voltage which is specified as 10 volts dc. With the specified excitation voltage, the angular acceleration sensitivity factor is given in appendix A as "5.7 $\mu V \cdot s^2/rad$." Generally, it is accepted practice to give associated test conditions for which the sensitivity applies, such as frequency and acceleration amplitude. No such information was supplied, therefore, the value of 5.7 $\mu V \cdot s^2/rad$ is interpreted as a nominal value. Phase response is inferred by the resonance frequency and damping factor and is discussed in the following section.

2.2 Frequency Response

The frequency response specification is given as "flat (to) within 1 dB to approximately 700 Hz." Transducers having a strain gage type sensing element usually have "dc response" (a frequency of zero hertz), however, because of a small, pressure-equalizing, bleed orifice in this design, the unit does not have dc response. Discussion with the manufacturer disclosed that the response at the low end of the spectrum is thought to roll off somewhere near 1 Hz or less [2]. Neither the manufacturer nor NBS has made measurements at this time to assess the low-frequency roll-off.

The nonlinear response with frequency is caused by the transducer's natural mechanical resonance which is given as about 2600 Hz. The rate of sensitivity increase as a function of frequency below the natural resonance is controlled by the damping. The preliminary specifications state that the "phase response" is "typical of an undamped system." With near zero damping, the response typically increases by about 4% to 6% at 20% of the resonance frequency. In this instance, one-fifth of the resonance is about 520 Hz.

Assuming that the transducer exhibits the typical behavior of other types of accelerometers, i.e., the mechanical resonant system can be

represented as a second-order, single-degree-of-freedom, spring-mass, lightly damped system, the response R can be predicted by the following relationship [3] where ω is the angular stimulus frequency and ω_n is the natural mechanical resonance.

$$R = \frac{1}{\sqrt{(1 - \omega^2/\omega_n{}^2)^2 + (2\xi\omega/\omega_n)^2}}. \qquad (1)$$

Further assuming a typical value for the fraction of critical damping of $\xi = 0.01$ (i.e., mechanical Q = 50)[2], the expected response is shown in figures 1A and 1B. The maximum response rise is consistent with the assumed mechanical Q of 50 as shown by figure 1A. Figure 1B shows the same function with the frequency one decade less than in figure 1A and also with the ordinate being greatly expanded. The computed rise at 700 Hz is about +7.8% (or +0.65 dB) as compared to the preliminary specification of +12% (+1 dB). It appears that the preliminary specification is conservative or that the damping factor may not be as assumed. The rise at 100 Hz is approximately +0.15% and at 300 Hz is approximately +1.3%. It is anticipated that the frequency spectrum of the angular acceleration to be measured in the final application (i.e., boxer's head motions) will not contain frequencies greater than several hundred hertz. This overall response is adequate to satisfy the demands for the transient bandwidth of the expected in measurement application.

The phase lag of the electrical output as compared to the mechanical input is predicted by [3]

$$\phi = \tan^{-1}\left[\frac{2\xi - (\omega/\omega_n)}{1 - (\omega/\omega_n)^2}\right]. \qquad (2)$$

Again, assigning values of resonance frequency of 2600 Hz and the fraction of critical damping of 0.01, the phase lags are 0.03° at 100 Hz, 0.13° at 300 Hz and 0.33° at 700 Hz. These are sufficiently small so as to be of no practical concern for the expected measurement application.

---

[2]The damping factor is related to mechanical Q by the relationship $\zeta = 1/2Q$. A mechanical Q of 30 to 100 is typical of most lightly damped accelerometer designs, therefore, Q = 50 is a reasonable approximation for purposes of these calculations.

2.3 Amplitude Linearity

The preliminary specifications give the amplitude linearity specification for this angular accelerometer as "...less than 1 percent nonlinearity..." This is interpreted as: the deviation at any amplitude from a least-squares linear-fit to the data within the transducer's range will be less than one percent of the reading. This is illustrated in figure 2.

2.4 Transverse Axis Angular Sensitivity

The preliminary specification for the response to transverse angular acceleration (i.e., input angular acceleration perpendicular to the sensing axis) is given as "3% maximum, 2% typical." This applies for all frequencies and amplitudes throughout the transducer's operating ranges.

2.5 Linear Acceleration Sensitivity

The response to linear input acceleration is given under two conditions: parallel to and perpendicular to the angular sensing axis.

2.5.1 Linear Acceleration Sensitivity Parallel to Sensing Axis

The preliminary specifications give the linear acceleration sensitivity parallel to the sensing axis as "2.5 rad/($s^2 \cdot g$) from dc to ≈ 50 Hz, increasing directly with frequency above ≈ 50 Hz at about 0.05 rad/($s^2 \cdot g \cdot Hz$)." This is shown graphically in figure 3. This can be expressed as

$$2.5 \text{ rad}/(s^2 \cdot g), \quad 0 \text{ Hz} \leq f \leq 50 \text{ Hz}, \text{ and}$$

$$0.5 \text{ rad}/(s^2 \cdot g \cdot Hz), \quad f > 50 \text{ Hz} .$$

Where plotted versus frequency, the linear sensitivity appears constant above 50 Hz if the ordinate units are rad/($s^2 \cdot g \cdot Hz$). Below a frequency of 50 Hz, the function increases as (1/f) because the specification contains no frequency term. This lower portion represents a constant response of 2.5 rad/($s^2 \cdot g$).

2.5.2 Linear Acceleration Sensitivity Perpendicular to Sensing Axis

The sensitivity for input linear acceleration which is perpendicular to the angular sensing axis "increases directly with frequency (at a rate of) 0.04 to 0.05 rad/($s^2 \cdot g \cdot Hz$)." This is shown in figure 3 by the dashed line below 50 Hz.

2.6 Physical Description

Figure 4 shows a photograph of the accelerometer. It is approximately 3 cm long with 0.5 inch hex faces to facilitate mounting. The integral mounting post is a UNF 1/4-28 external thread. Without the connecting cable, the accelerometer's center-of-gravity was measured on a knife edge as approximately 8.9 mm (0.35 in.) from the base. The manufacturer gave [2] the location as about 7.6 mm (0.30 in.) from the base. The illustration of figure 4 shows the location for the center-of-gravity for the orthogonal planes and is located symmetrically on the cylindrical axis of the accelerometer. The measured mass of the accelerometer (without the electrical cable and connector[3]) was 16.5 ±0.1 grams.

The electrical connections were made through a supplied cable having a miniature six-pin connector. The "pig-tail" leads are color coded and were tagged with the following information:

Cable Lead	Tagged Information	Comment
Red	"Input +"	Bridge excitation
Black	"Input -"	Bridge excitation
White	"Output +"	Signal output, high
Green	"Output -"	Signal output, low

The principle of operation in its simplest form can be described as a liquid filled torus having an intercepting diaphragm. As the torus is accelerated about an axis perpendicular to the toroidal plane, a differential pressure is exerted on the diaphragm. Strain gages are mounted on the diaphragm and hence sense the differential pressure which, in turn, is directly proportional to the angular acceleration.

3. LABORATORY MEASUREMENTS

The laboratory measurements selected for this assessment can be divided into three sets:

A. Transducer resistance measurements,
B. Angular acceleration measurements, and
C. Linear acceleration measurements.

The resistance measurements were preliminary to all the others to ensure that all leads and transduction elements were intact. The angular acceleration measurements were designed to assess the most

---

[3]For mass considerations, the accelerometer is measured alone. The connector has a mass of about 1 gram. In most applications, only a portion of the cable dynamically loads the accelerometer as effective mass; generally about 2 cm of cable length (i.e., about 0.5 gram) is added to account for the cable's effective mass.

important transducer parameter, its angular sensitivity factor, along with the frequency response and amplitude linearity. The linear acceleration measurements were designed to evaluate the transducer's output when rectilinear motion is applied to the angular accelerometer. Ideally, the output should be zero under the latter conditions and any output is interpreted as an error.

This section contains descriptions and discussions of the test philosophy, test systems and apparatus special fixtures, test procedures, data collection and presentation, and data analysis and discussion. Measurement results of weight and center-of-gravity were given in section 2.6 of this report.

3.1 Resistance Measurements

The "lead-to-lead" resistance was measured for an unmounted accelerometer to ensure that no damage had occurred in the leads, connector, and transducer gages. A dc digital ohmmeter was used to measure the resistances. The resistance was measured with the ohmmeter leads in a "forward" and "reversed" position to check for any possible "polarity" effects. Table 1 gives the measurement results. The resistance ranged from about 1200 to 1670 ohms. There was no apparent ohmmeter-lead reversal effect; the "reversed" reading agreed with the "forward" reading to within 0.2 ohm in the worst case. The resistance from the shield to any other lead was an open circuit insofar as the ohmmeter reading indicated. The resistance from the "pig-tail" end of the shield wire and the transducer case was approximately 0.5 ohm.

The computed current drain with a 10 V dc excitation voltage applied between the ±INPUT leads would be 5.991 mA. The measured current with 10.000 V dc applied was 5.912 mA, or a difference from the computed value of about -1.3%. The accelerometer was held in a hand for several minutes and the current monitored; the "warm" current was 5.879 mA (about 0.6% lower than the previous ambient temperature current). This would indicate that the overall resistance between the ±INPUT leads was temperature sensitive and that self-heating and external environmental heating can be expected to cause resistance changes of perhaps several percent. The temperature coefficient of bridge resistance was obtained from the manufacturer [4] as approximately +0.7% per degree C (0.4% per degree F) as measured at any pair of diametric points on the bridge.

With ±10 V dc applied between the ±INPUT leads, the dc offset (bridge unbalance) voltage was measured as 9.22 mV under ambient laboratory temperature conditions. This indicates that the electrical balance of the strain gage bridge elements is rather good (within about 0.09%). The unbalance as a function of temperature was not measured, but should be if further testing is performed at a later time.

3.2 Angular Acceleration

3.2.1 Test Philosophy

With a known angular acceleration applied to the transducer along its sensitive axis, the accelerometer's transfer function (i.e., sensitivity factor) can be determined by measuring its electrical output. This simple relationship is shown below.

$$\text{Sensitivity Factor} = \frac{\text{Voltage Output}}{\text{Acceleration Input}}$$

The units of the sensitivity factor are volts per unit angular acceleration, or $V/(rad/s^2)$. The preferred form of expressing these units is $V \cdot s^2 \cdot rad^{-1}$ and will be used throughout this report.

Further, the sensitivity factor is directly proportional to the bridge excitation voltage. For all of the measurements made herein, the bridge excitation voltage was nominally 10 V dc.

3.2.2 Electrical Excitation Power Configuration

The electrical excitation for the resistance bridge was supplied from two separate adjustable and regulated sources. This is shown schematically in figure 5. The two power sources were connected in series so that the sum of the two voltages is the bridge excitation voltage, nominally 10 V dc. The center connection of the sources is connected to the system ground. For nominally equal bridge resistance and no input angular acceleration, the bridge output voltage is zero. Because the four bridge arms are not all exactly equal, there is a small residual unbalance (offset) voltage. The two power supplies were adjusted so that the sum of their two voltages always equaled 10 V dc and the two output voltages to ground were opposite and equal. This procedure thus minimizes the dc voltages at the output terminals of the bridge. This was necessary to avoid dc overloading of sensitive amplifiers used in the measurement of the small ac signal outputs.

3.2.3 Laboratory Instrumentation, Amplifiers, and Filters

The electrical output from the accelerometer is a small ac voltage from a source impedance of about 1500 ohms. Even with moderately good shielding and low noise power supplies, noise and hum (i.e., 60 Hz related components) make accurate measurements difficult. The nominal sensitivity given for the accelerometer was 5.7 $\mu V \cdot s^2 \cdot rad^{-1}$. The test acceleration amplitudes to be used ranged from about 64 to 5000 rad/s^2 peak. (Details of the input acceleration are discussed in a later portion of this report.) Multiplying the sensitivity and the angular accelerations provides

estimates of the voltages to be measured. For sinusoidal input accelerations, the output voltages could be expected to range from about 0.26 to 20.1 mV rms. To ensure adequate precision and accuracy, the voltage measurement resolution and uncertainties should be a fraction of a percent; this requires that low-level ac signals (at low frequencies at times) must be known to within a few microvolts.

Narrow band amplifiers were used as is shown in figure 6. The output of the accelerometer was fed into a preamplifier/filter with differential inputs. Low noise gains of nominally 200 or 500 were achieved in the first amplifier. Some band-pass filtering was also achieved in this preamplifier. Its output fed two cascaded filters, each having nominally 0 dB gain (unity gain). These filters, identified as "filter A" and "filter B" in figure 6, could be configured as low-pass, high-pass, band-pass, or band-reject filters. The output of filter B was connected to a digital measuring system which measured and oscilloscopically displayed the signal.

Because the measurement system includes amplifiers and filters, the response of the external system must be removed from the measurement to assess the transducer performance. This is shown as

$$\text{Transducer Signal} = \frac{\text{Measured Signal}}{\text{External Gain}} .$$

Because the gain settings of each of the amplifiers and filters were only known nominally, and further modified by the "skirt response" of the filters, system gain had to be measured for each of the gain- and filter-setting combinations used in the measurements.

3.2.4 Angular Acceleration Generation

The input angular acceleration to the accelerometer was generated by a dual spin-axis rate-table (DSART). This device consists of two motor-driven platforms whose rotational axes are perpendicular and intersect. The main platform is oriented horizontally and rotates about a vertical axis. Mounted on this horizontal platform is a second motor and platform whose axis is oriented horizontally. Figure 7 shows a simplified drawing of the DSART platforms. Each of the two motors is independently controllable and each of the angular velocities is measurable. When both motors are rotating at a constant speed, an angular acceleration is generated about the vertical axis which is sinusoidal and predicted from

$$\alpha(t) = \omega_1\omega_2 \sin(\omega_2 t + \Theta_2), \qquad (3)$$

where $\alpha(t)$ is the angular acceleration, ω_1 is the angular velocity of the horizontal platform, ω_2 is the angular velocity of the second platform, and t is a generalized unit of time. The phase angle θ_2 is the angle between some arbitrary rotational reference position on the upper platform and the accelerometer sensing axis, and is generally selected such that $\theta_2 = 0$ and can thus be neglected. An accelerometer mounted on the upper platform, such that its sensitive axis is perpendicular to the upper motor's horizontal axis, will experience input angular acceleration as described by eq (3). (References 5 through 7 give details of the DSART operation and theory.)

The lower main platform is servo-controlled so that its angular velocity is constant and is selected by a set of thumbwheel switches on the DSART's front panel. It incorporates an optically sensed, multi-slit disc in the velocity sensing servo-control circuit. The velocity is selectable over a range from 0.0001 to 3200 °/s (about 1.7 μrad/s to 56 rad/s).

The upper motor is not servo-controlled and its velocity is set manually by a multi-turn control. The velocity is sensed by a 60-tooth circular gear and the output from the magnetic pickup is fed into an electronic counter. The counter reading is in units of revolutions per minute (rpm) when the counter is gated at 1 second. Greater velocity revolution can be obtained by gating the counter to 10 or 100 seconds.

As given by eq (3), the peak amplitude of the angular acceleration is calculated by the product of the two angular velocities, ω_1 and ω_2. Because the two velocities are in mixed, non-metric units, a factor is needed to convert the product of degrees per second and revolutions per minute to radians per second squared. (The factor also accounts for the two factors of 2π.) Hence,

$$\alpha_{pk} = \left(\frac{\pi^2}{5400}\right) \nu_1 \nu_2 \text{ rad/s}^2, \tag{4}$$

where ν_1 is the angular velocity of the lower platform in units of degrees per second and ν_2 is the velocity of the upper platform in units of revolutions per minute. For convenience, the angular accelerations, α_{pk}, are peak accelerations and hereafter will be designated as α, without any subscripts.

Table 2 shows the angular velocities needed to generate the angular accelerations at specified frequencies. Note from eq (3) that the sinusoidal frequency of the acceleration is determined by the velocity of the upper motor, as

$$f = \frac{\nu_2}{60} \text{ Hz}, \tag{5}$$

where ν_2 is in units of rpm. The frequencies shown in table 2 were selected so that they are evenly spaced on a logarithmic scale.

The upper motor loses velocity stability at rates below about 100 rpm (10.5 rad/s); its maximum velocity is specified as 6000 rpm (628 rad/s). Therefore, the maximum usable frequency range over which the DSART operates is about 1.67 to 100 Hz. The maximum angular acceleration, because of bearing loading forces, is 7896 rad/s^2 peak[4]. These limiting parameters (i.e., ν_{1max} = 3200 °/s, ν_{2max} = 6000 rpm, and α_{max} = 7896 rad/s^2) then set the limits of operation for the DSART. The values shown in table 2 are all within these limits and can be derived from eqs (4) and (5).

In practice, all the frequencies and accelerations may not be obtainable because of problems of unbalance, noise, hum pickup, mechanical resonances, wave distortions, or motor heating. Balancing becomes a critical and limiting factor as the test frequencies increase (i.e., as ν_2 increases). Mechanical vibration and, hence, mechanical "noise" results from unbalanced conditions. Two-plane balancing is required on each end of the rotating test specimen, usually with weight increments as small as 0.5 gram.

At low velocities of the upper motor, the driving torque is very small. Under these conditions, interactive forces between the main platform's rotation and the upper motor's rotation cause coupled torques to exist which can distort the desired sinusoidal motion; that is to say that the upper motor cannot maintain a constant angular velocity but is modulated by gyroscopically coupled torques which exist because of the lower platform's rotation. When distorted motions occur, the peak value of angular acceleration can no longer be predicted simply by eq (4).

The slip rings used to conduct the signal from the rotating platform are also a source of electrical noise. The lower rings are low-noise, mercury-wetted rings; the upper rings have simple dual carbon brushes. The latter are orders of magnitude more noisy than the mercury-wetted rings. The noise from the carbon brushes tends to be in bursts of high frequency signals, the bursts being synchronized with the rotation of the upper motor. Electronic filtering is relatively effective in minimizing the brush/ring noise.

---

[4]The manufacturer limits the maximum operating acceleration by specifying that the product of the two angular velocities in rpm shall not exceed 720 000 (rpm)^2.

Sixty hertz pickup hum is also a source of noise which contaminates the acceleration-generated transducer signal. The principal source of 60-Hz hum is from inadequate shielding and the location of wiring within the DSART cabinet. The wiring passes close to a power transformer within the DSART frame. Electronic filtering can be effective in attenuating these hum components at most frequencies of test; however, acceleration tests at 50 Hz were not possible because the filters could not be adjusted to provide sufficient attenuation at 60 Hz.

3.2.5 Test Measurements

3.2.5.1 Angular Acceleration Sensitivity

The angular accelerometer to be tested was mounted onto the upper rotating platform of the DSART illustrated in figure 7. The center-of-gravity of the accelerometer was located approximately 3 mm above the horizontal axis of the upper platform and was in line with the vertical axis of the lower platform. The cable was coiled and secured to the upper platform to prevent any whipping action. The upper platform was balanced so that minimum unbalanced vibration occurred over the rotational speeds from about 100 to 6000 rpm.

As shown in figure 6, cascaded filters and amplifiers were used to minimize the noise and to increase the signal voltage to a level suitable for digital measurement. Because the filter settings were often close to the test frequencies, the amplifier gain response was on the filter "skirts" and the nominal gains as indicated by the amplifier settings were not accurate enough for these measurements. Therefore, the cascaded gains were measured at each of the test frequencies and the gain slope with frequency determined. In practice, an exact frequency could not be set accurately nor maintained for more than short periods because of the speed variations and drifts of the upper DSART motor. The velocity, ν_2, could be measured but would differ slightly from the nominal setting. It was thus necessary to make slight frequency corrections to the amplifier/filter gains. Table 3 gives the nominal test frequencies, the measured gain, the gain slope, and the filter settings.

The signal outputs from the amplifiers and filters went into a digital measuring system with averaging and data processing capabilities. Random components of noise, jitter, and some distortions were removed from the signal by ensemble averaging of a number of waveforms. The number of ensembles ranged from 10 to 100, but usually numbered 25 or 50. The ensemble averaging has the effect of a low-pass filter.

After averaging the signal, it was integrated over a whole number of sinusoidal cycles to determine and remove by calculation any dc voltage components contributed by the amplifiers. The rms value of the waveform was determined and used as a basis for calculating the transducer sensitivity. As shown in section 4.2.1 of this report,

the sensitivity is the ratio of the electrical output divided by the mechanical input. The sensitivity factor, S, was computed by the use of the following relationships:

$$S = \frac{\sqrt{2}\ 5400\ E}{\pi^2 \nu_1 \nu_2\ H_n [1 + 0.01\ c(f_t - f_n)]} \quad \mu V \cdot s^2 \cdot rad^{-1}, \qquad (6)$$

where E is the rms voltage output from filter B, H_n is the measured gain at the nominal frequency, c is the gain slope in units of percent per hertz and the other parameters are as previously described. The factor of $\sqrt{2}$ is a simple conversion from rms voltage to peak voltage for a sinusoidal waveform; this is necessary inasmuch as the acceleration is in peak units. The frequencies, f_t and f_n, are the test frequency and the nominal frequency, respectively. The bridge excitation voltage was maintained at 10 V dc for all the measurements.

At each test frequency and acceleration, a minimum of three measurements were taken to compute the sensitivity factor. In some instances considerably more than three sets of data were taken.

Figures 8 through 17 show the results graphically with the measured sensitivity plotted versus frequency. The measured points are represented by an asterisk (*) and the group average frequency and average sensitivity are shown by the symbol "O." The left-hand ordinate is the measured sensitivity plotted from 5 to 6 $\mu V \cdot s^2 \cdot rad^{-1}$; the right ordinate is the percentage deviation referenced to value of sensitivity of 5.529 $\mu V \cdot s^2 \cdot rad^{-1}$. (This value was chosen from an early set of data at 15 Hz and at 1000 rad/s^2 because the scatter in data is small at these operating conditions. The value is arbitrary and has no special significance, but serves as a common level for comparison purposes.)

The accompanying tables of appendix B for the figures B-1 through B-10 give the average frequency, average sensitivity, the percentage deviation, and the number of measurements for each of the data sets by frequency. Figure 8 is the summary of all the angular acceleration sensitivity measurements for accelerations from 64 to 5000 rad/s^2. Overall, there are 229 measurements that are summarized in figure 8. For example, at a frequency of 70 Hz, there are 62 data points plotted.

The average of the data as plotted in figure 8 indicates that the transducer frequency response is relatively "flat" to within about ±2.5% over a frequency range from 1.5 to 70 Hz. There is a general trend for the data to have an apparent increase in sensitivity as frequency increases. The reasons for this are unknown. Theoretically, the sensitivity rise should not be more than a small fraction of one percent at 100 Hz (see fig. 1B). Without further testing, one cannot state that the rise is a result of transducer performance, but rather

could be a result of systematic error in the measurement apparatus or procedure.

3.2.5.2 Amplitude Linearity Measurements

The data collected and presented in the previous section (angular acceleration sensitivity) were regrouped and analyzed for amplitude response. The data at each acceleration amplitude was averaged to get a single value regardless of frequency. This is plotted and shown by figure 9. The averaged data are shown by the plotting symbol "1." The straight, sloped line is a first degree regression fit to these data. The fit line is difficult to detect because it is very close to the data, however, a slight difference can be seen at 2000 rad/s^2. Figure 10 shows the same data in terms of deviation from the mean accelerometer sensitivity (slope of fit curve of fig. 9) rather than accelerometer output voltage. Here, the differences between the measured and fit values are more apparent. The maximum difference allowable by the preliminary specification is ±1% (see appendix A and section 2.3 of this report). Table 4 gives tabular results in terms of the measured accelerometer sensitivity. The column headed percentage deviation should be less than ±1% to meet the specifications. The largest difference measured was approximately -1.27% at 500 rad/s^2.

It should be noted that other effects are present and "contaminate" the data to an unknown amount. For example, there was no attempt to separate the frequency response effect from the amplitude response when examining the amplitude linearity. With the present data, the frequency effect, which is included, has the tendency to make the amplitude linearity appear worse than it would be at a single frequency. Data from the test frequencies of 70 and 100 Hz are included in this analysis. It was seen from the angular acceleration sensitivity that the tests at 70 and 100 Hz tended to be of a greater-than-expected sensitivity. It is believed that this same "data rise" at these two frequencies may have "biased" the linear fit slightly higher than it should be. Therefore, the value of -1.27% deviation at 500 rad/s^2 is probably not as significant as it would first appear. Furthermore, other measurement uncertainties are associated with each of the datum points shown which could easily account for the apparent "greater-than-specification" deviation.

It should also be further noted that the analysis was accomplished and acceleration data were taken at only 10% of the transducer's full scale of 50 000 rad/s^2; no statement can be made concerning the response for acceleration amplitudes between the 5000 rad/s^2 level to which testing was done and the full-scale range of 50 000 rad/s^2.

3.3 Transverse Axis Angular Sensitivity

The sensitivity of the accelerometer to angular accelerations applied in a direction which is transverse to the main sensing axis was not

performed directly. Indirect measurements of the influence of a transverse angular sensitivity on the performance are discussed below.

With the accelerometer mounted on the DSART upper platform as previously described, a component of transverse angular motion is present by the fundamental operation of the DSART. Equation (3) shows a phase term, θ_2, which, for the previous set of measurements, was set to zero. When set to zero, the mechanical rotational reference position is aligned in the same direction as the accelerometer sensing axis. Under these conditions, a second component of angular acceleration exists on the upper platform which is in quadrature, i.e., it occurs at a mechanical rotation of 90° later. This component has the same angular acceleration, sinusoidal amplitude, $\omega_1\omega_2$, but a phase angle of $\pi/2$ rads or 90°. Thus there exists, by the fundamental operation, a quadrature motion (i.e., transverse) which is of the same amplitude as the main, in-phase angular acceleration. So while the accelerometer is sensing the "in-axis" angular acceleration generated by the DSART, it is also simultaneously experiencing a transverse angular acceleration of equal amplitude (i.e., 100% transverse input).

In theory, if the accelerometer's phase response is accurately measured, and the in-phase and quadrature-phase components resolved, then the transverse sensitivity could be measured; the transverse sensitivity would be the quadrature-phase component. This, in practice, however, is not easy. Phase shifts in the measuring system and transducer have to be carefully determined. For example, if the transverse sensitivity were at a typical value of 2% of the main angular sensitivity, the phase shift in response due to 100% transverse input as described above calculates to be only 1.1°. Phase shifts due to the accelerometer resonance (see eq (2)) and, more importantly, due to the amplifiers and filters would have to be known very precisely. This is especially difficult when the filters are used at frequencies near their cutoff frequencies.

A second method was considered, but the lack of time did not allow it to be tried. If the accelerometer sensing axis were aligned in the same direction as the rotational axis of the upper platform, then, ideally, the angular acceleration in this direction would be zero. The accelerometer would experience 100% transverse input motion from the main acceleration vector of the upper platform. Again, ideally, the output measured under these conditions represents the transverse sensitivity of the transducer. This assumes, of course, perfect alignments of the accelerometer mounting, DSART rotational axes, etc. It also assumes that the velocity, ω_2, of the upper platform is perfectly constant, and that no variations in velocity occur over a one revolution. Observation has shown the later condition is not true because of coupled gyroscopic torques between the two rotating systems, namely, the lower and upper platforms and their drive systems. The upper platform does not maintain a

constant velocity, especially at low velocities when waveform distortion is easily observable. Velocity variations of the upper platform are indeed angular accelerations in that axis. At higher velocities, the electric drive motor develops sufficient torque to overcome the gyroscopic coupled torques. Also, the angular momentum is much greater which tends to "smooth out" the variations in angular velocity.

It should be kept in mind that the angular transverse sensitivity is a small quantity, i.e., about 2% of the main sensitivity; therefore, signals in the order of 2/100 of 5 $\mu V \cdot s^2 \cdot rad^{-1}$ are being sought. This alone represents a difficult measurement. Moreover, the gyroscopically coupled torques occur at the same period (or frequency) as the transverse acceleration input vector to the accelerometer, since both are directly related to the rotational velocity of the upper platform. Hence one cannot easily separate the effects of true transverse response and upper platform velocity variation (i.e., angular accelerations). Transverse sensitivity would better be performed on a specially designed apparatus expressly made for the purpose.

3.4 Linear Acceleration Testing

3.4.1 Test Philosophy

Two specifications for linear vibration sensitivity are given by the preliminary specifications; one for input vibration parallel to the angular accelerometer's sensing axis, and the second for vibration perpendicular to the angular sensing axis. These specifications were discussed in section 2.5 of this report.

The ideal angular accelerometer would have zero output for purely rectilinear input vibration. Any accelerometer output under these conditions represents an error. Testing for these angular accelerometer characteristics is complicated by the fact that pure rectilinear motion does not exist on even the best of linear vibration exciters (shakers). Cross axis motion as well as rocking modes always are present to some finite level; the rocking modes generate angular accelerations. Furthermore, the rocking modes change with frequency, drive amplitude, position, direction, mass, and sometimes temperature and time. It is, therefore, not only a difficult measurement, but one that often has little meaning unless extreme care has been taken by very elaborately accounting for rocking modes of the linear exciter.

The fixture to which the accelerometer was mounted was made and mounted so that it and the accelerometer represented a moment balanced load to the exciter, i.e., the exciter was driving its linear acceleration vector through the effective center-of-gravity of the fixture and accelerometer combined. The fixture was a 2.5 cm cube-shaped block of aluminum machined square so that perpendicularity was ensured. A UNF 1/4-28 hole was tapped to accommodate the integral

mounting stud of the accelerometer (see fig. 4). Various UNF 10-32 threaded holes were located so that the block could be attached to the linear exciter in a balanced manner.

The electrical and instrumentation hookups were the same as previously described for the angular acceleration tests (see section 3.2.2). The filters were set for a band-pass configuration as follows (see fig. 6): preamplifier/filter gain was 1000 and filters set to 3-Hz high pass, 10-kHz low pass; filters A and B gains were 0 dB and filters set to 5-Hz high pass and 2-kHz low pass, respectively. Therefore, the overall gain was nominally 1000 (+30 dB) with a band pass of approximately 5 to 2000 Hz. Because measurements were taken at least one octave away from each of the band limits, gain measurements were not made as they were for the angular acceleration tests. Furthermore, accuracy was not paramount for these linear acceleration tests so accurate gain was not necessary.

3.4.2 Linear Sensitivity Parallel to Sensitive Axis

The accelerometer was mounted on the linear vibration exciter so that the linear sinusoidal acceleration vector was aligned parallel to the angular acceleration sensitivity axis. Linear accelerations were servo-controlled to a constant peak amplitude of nominally 50 m/s^2 (5 g peak). The test frequencies were manually selected and ranged from about 25 Hz to 1000 Hz.

The linear sensitivity is referenced to the angular sensitivity by the following relationship.

$$S_\ell = \frac{\sqrt{2}E}{A_\ell H S_a} \text{ rad}/(s^2 \cdot g), \tag{7}$$

where

S_ℓ is the linear acceleration sensitivity in units of $\text{rad}/(s^2 \cdot g)$ (same units as given in the preliminary specifications),

E is the rms output voltage from the amplifier and filters (the term $\sqrt{2}$ converts the rms values to a peak value).

A_ℓ is the linear acceleration test amplitude in units of "g" (1 g = 9.80665 m/s^2),

H is the composite amplifier gain, and

S_a is the angular acceleration sensitivity factor in units of $\mu V \cdot s^2 \cdot rad^{-1}$.

For these tests, the following parameters were set:

A_ℓ = 5 g peak (approximately 50 m/s^2),

H = 1000 (+30 dB), and

S_a = 5.529 $\mu V \cdot s^2 \cdot rad^{-1}$ as determined from the angular acceleration sensitivity.

Table 5 gives the measurement results over a frequency range from about 25 to 700 Hz. A rocking mode resonance in the exciter prevented measurements at higher frequencies. Figure 11 shows the results graphically along with the preliminary specification which is also plotted.

Because of the angular accelerations present in the linear exciter's motion (rocking modes), this data may not represent the true response of the accelerometer, but rather the combined response of the exciter and the accelerometer. The rocking motion adds vectorially to the linear sensitivity since the exciter's rocking or "contamination components" could either add to or subtract from the true response. This is probably the cause of the "peak-valley" response seen at 200 and 300 Hz in figure 11. Further, the rise in response beyond 700 Hz is very probably due to a known rocking resonance in the exciter near 1000 Hz. Even so, the measurement results indicate that the linear acceleration sensitivity parallel to the angular sensing axis is low and probably within the manufacturer's preliminary specifications.

3.4.3 Linear Sensitivity Perpendicular to Sensitive Axis

The accelerometer was mounted on the adaptor block which was, in turn, mounted onto the vibration exciter so that the linear sinusoidal acceleration vector was aligned perpendicular to the angular accelerometer's sensitive axis. As before, the linear accelerations were servo-controlled to a peak amplitude of 50 m/s^2 (5 g peak). The frequencies were manually selected and ranged from 100 to 1000 Hz.

The linear sensitivity perpendicular to the angular sensing axis is referenced to the angular sensitivity by the following relationship.

$$S' = \frac{S_\ell}{f} = \frac{\sqrt{2E}}{A_\ell H S_a f} \quad rad/(s^2 \cdot g \cdot Hz), \tag{8}$$

where

S' is the linear acceleration sensitivity in units of $rad/(s^2 \cdot g \cdot Hz)$ (same units as given in the preliminary specifications),

E is the rms output voltage from the amplifiers and filters (the factor of $\sqrt{2}$ converts the rms voltage to peak voltage),

A_ℓ is the linear acceleration test amplitude in units of "g" (1 g = 9.80665 m/s^2),

H is the composite amplifier gain,

S_a is the angular acceleration sensitivity factor in units of $\mu V \cdot s^2 \cdot rad^{-1}$, and

f is the test frequency in Hz.

For these tests, the following parameters were selected:

A_ℓ = 5 g peak (approximately 50 m/s^2),

H = 1000 (+30 dB) or as noted in table 7, and

S_a = 5.529 $\mu V \cdot s^2 \cdot rad^{-1}$.

Equation (8) is the same as eq (7) except for the new term of frequency, f, in the denominator.

When the angular accelerometer is mounted in the configuration as described, the angular sensing axis is perpendicular to the linear acceleration vector, however, rocking motions on the exciter (i.e., angular accelerations) are aligned with the angular sensing axis. The importance of this cannot be overstated inasmuch as very small rocking motions are directly sensed by the angular accelerometer. In order to perform this measurement satisfactorily, one would have to ensure that the exciter's rocking motions were indeed extremely small. For example, at A_ℓ = 5 g and at f = 100 Hz, the rocking mode angular acceleration would have to be less than about 2.5 rad/s^2 in order to have negligible effect on the linear sensitivity measurement; this is considered to be a low angular acceleration. Another way to illustrate these small motions in a way more familiar to those working with rectilinear vibration is to relate an equivalent angular acceleration in terms of a linear acceleration. If, as in the case above, the angular acceleration were to be limited to 2.5 rad/s^2 at 100 Hz on a vibration exciter having a table about 7.5 cm (3 in.) in diameter, the maximum permissible difference in vertical linear accelerations

between the two edges of the table could be only about 0.00004 g peak, small indeed, and would in itself represent a difficult measurement.

The measurements given below represent a first attempt at obtaining some measure of linear sensitivity. Because of the above rocking mode considerations and restraints, good quality measurements could not be obtained. Time and funds did not permit the development of a method by which better measurements could be achieved. Table 6 gives the measurement results over a frequency range from 100 to 700 Hz. Figure 12 shows these results graphically.

One set of measurements was taken and evaluated by the use of eq (8). The accelerometer's angular axis was oriented in an approximate "cross-trunion" direction on the exciter. A second set was done by rotating the accelerometer 90° about its angular sensitive axis and the measurements repeated. The results of both sets of data as measured are two to four times greater than the preliminary specifications, however, it is felt that under these test conditions, the fault likely lies with the testing exciter and method, and not with the accelerometer. The fact that the results are this close to the specification is regarded as a probable indication that the accelerometer's linear sensitivity is low and in the order of the preliminary specification (i.e., 0.05 rad/(s^2·g·Hz)).

3.4.4 Other Effects

While performing the measurements for the linear sensitivity with the acceleration perpendicular to the angular sensing axis (see section 4.4.3), distortion was observed in the waveform. Nominally, the waveform should have been sinusoidal, however, higher order harmonics were present.

A swept frequency response was made over the frequency range from about 200 to 3000 Hz and is shown in figure 13. The unfiltered accelerometer output is plotted versus frequency. The output was low and relatively flat at the lower end of the spectrum up to frequency of about 1425 Hz. Several resonance rises are noted about 1425 Hz, the most notable being at a frequency of about 2160 Hz. This resonance was traced to the connector and top of the accelerometer case. Dwelling at this frequency, large effects could be seen on this high Q resonance by lightly touching the connector. This resonant motion, probably coupled through the electrical leads, caused an output from the strain gage sensing elements.

Because this resonance is such a high Q, it can easily be excited by subharmonically related accelerations which can have the effect of seriously distorting the waveform. In the present accelerometer packaging configuration, this may cause application measurement problems. If, however, the transducer is repackaged for the DoT application in a miniature triaxial configuration, then this case top/connector resonance would not likely exist. Any new configuration should be tested to ensure that similar resonances do not exist.

3.5 Measurement Uncertainties

The uncertainties in the measurement process stem from various sources, some of which are evaluatable, but others which are more difficult to ascertain. A rigorous error analysis was not performed inasmuch as to do so could consume more effort than did the measurements themselves. The errors which are more obvious and evaluatable are discussed below and combined to obtain some reasonable measure of uncertainty in connection to the data shown previously.

3.5.1 Bridge Voltage Excitation

The output voltage from the four-arm Wheatstone bridge within the transducer is directly proportional to the bridge excitation voltage and, moreover, uncertainty of the output voltage is directly proportional to uncertainty of the excitation voltage. The voltage was adjustable and measurable to within a resolution of ±0.02% with an additional uncertainty of ±0.05% in the voltage magnitude. Voltage drops in the short leads and connections were neglected. Therefore, the total estimated uncertainty in the bridge excitation voltage is ±0.07% worst case (direct addition) and ±0.054% (rounded to ±0.05%) root-sum-squared (rss).

3.5.2 Signal Voltage Measurement

The amplified and filtered output voltage was measured with a digital processing oscilloscope whose digitizing resolution was 10 bits; this translates to approximately ±0.1% of a full-scale digital word of 1 bit in 1024 bits. The ranging sequence was in a 1-2-5 scheme where it would be possible to measure at 2/5 of full scale before being able to down range to the next lower scale. This effectively makes the measuring resolution 2.5 times less than at full scale, or 2.5 x (±0.1%) = ±0.25% of reading. It is estimated that the integration process for dc voltage removal is accomplished to within ±0.05%. The rms voltage integration, squaring, summing, etc., is done to within ±0.1%. The ranging, gain, and reference voltage is known to within ±0.1% and the readout resolution is to five digits making its uncertainty about ±0.01%. Thus the overall voltage measuring uncertainty is estimated to be ±0.51% worst case and ±0.29% root-sum-squared.

3.5.3 Amplifier Gain and Filter Response

The amplifier gain was determined using a precision Kelvin-Varley divider whose setting resolution (because of noise and drift) was about 5 parts in 2000, or ±0.25% of setting. (The uncertainties associated with the divider ratio are in the order of a few parts per million (ppm) and are completely overshadowed by the lack of resolution due to system noise.)

The gain as a function of frequency was determined over a narrow band (usually a few hertz) around a nominal frequency to determine the gain slope with frequency. Referring to eq (6) (section 3.2.5.1 of this report), two other terms are seen, namely, the gain slope and frequency difference. Analysis of gain measurement data led to the conclusion that the overall effects of gain measurement, frequency, gain slope, noise, and drifts yielded an uncertainty of about ±0.75% worst case and about ±0.43% root-sum-squared.

3.5.4 Acceleration Determinations

The angular acceleration generated by the DSART is principally a function of the two angular velocities, ν_1 and ν_2, as shown in eq (6). The velocity, ν_1, of the lower platform has a setting accuracy of ±0.25%, a "wow and flutter" specification of 0.1% at 1/10 of full-scale range, and a stability specification of ±0.1%. These combine to be ±0.45% worst case and ±0.29% root-sum-squared.

The velocity, ν_2, of the upper platform is measured by use of a 60-tooth tachometer utilizing an electronic counter. At frequency of 1.5 Hz (90 rpm), the counter resolution over a 10-second counter gate time is ±1 part in 900, or about ±0.1%. Examination of the data indicates that drifts and other instabilities account for approximately ±0.48% uncertainties. Combining these sources of error, the worst case uncertainty is estimated as ±0.59% and ±0.49% for the root-sum-squared estimated uncertainty.

The angular acceleration is the product of the two angular velocities, therefore, the uncertainty in acceleration is approximately the sum of the uncertainties of each of the velocities. Combining these uncertainties leads to an estimate of the uncertainty for angular acceleration of ±1.04% worst case and ±0.74% root-sum-squared.

There are other sources of error in the acceleration prediction such as nonsinusoidal waveform distortion, or rocking motions of the DSART mechanisms which appear as angular accelerations; these effects are not evaluated here. However, some of the influences that those sources have on the uncertainty have been included in the final uncertainty value and are shown in section 3.5.7. In some instances, these "other sources" of uncertainty may not necessarily be small in comparison to those values given above. (If future work is performed using this hardware, efforts should be made to evaluate such errors and, if possible, reduce them.)

3.5.5 Computation and Arithmetic Errors

Calculations were performed digitally to 20-bit precision and read to 4 decimal places. Final values are reported and discussed to 3 decimal places, therefore, rounding errors can be interpreted as ±1/2 part in 550 parts, or about ±0.09% of the typical sensitivity reading.

3.5.6 Other Error Sources

There are a number of sources of additional errors leading to measurement uncertainty. A few of the more elusive parameters are noise and hum, nonsinusoidal distortion, cross-axis excitation and response, temperature changes, DSART rocking motions, etc. These sources could represent difficult and complex error relationships which are interdependent on frequency, acceleration, temperature, and mounting position as well as other now unknown quantities. In order to get a first order assessment of these effects, the scatter of the sensitivity measurement results was briefly analyzed. Because it is believed that the amplitude nonlinearities are small, the analysis was done on a frequency-by-frequency basis. Statistically, an estimate of the standard deviation was calculated for each set of data by frequency. The results are shown in table 7. The estimated standard deviation did not exceed ±3.5% for the 229 sets of data analyzed. This value is a measure of the scatter in the measurement process as a result of some of the sources discussed previously as well as some of the effects such as noise, distortion, cross-axis excitation, etc., which were not assigned values of uncertainty. For this analysis, a value of ±3.5% uncertainty is included in the error analysis to account for the observed scatter due to unevaluatable causes.

3.5.7 Combined Uncertainties

The uncertainties discussed above are summarized below. The "symbols" refer to the parameters as given in eq (6). The uncertainties given are for the worst case combinations.

Symbol	Source of Uncertainty	± Uncertainty %
-	Bridge excitation voltage	0.07
E	Measured voltage, rms	0.51
H,c, (f_t-f_n)	Amplifier gain, gain slope and frequency difference	0.75
ν_1, ν_2	Arithmetic calculations and round-off	0.09
α	Applied angular acceleration	1.04
-	Scatter and other effects	3.5
	Worst case sum	±5.96%
	Root-sum-squared	±3.76%

The worst case combination is about ±6% while the root-sum-squared estimate is about ±4%. In examining the foregoing data as summarized in figure 18, most of the data falls within a band of ±6% except

perhaps the data at 100 Hz. It is felt that other causes were affecting this data, to an extent beyond the error analysis. Overall, an estimated uncertainty of ±6% is acceptable as a realistic value in lack of a more thorough analysis.

All of the parameters listed above except the last, "scatter and other effects," are uncertainties which pertain to the test and calibration equipment, and not to the performance of the accelerometer. A portion of the accelerometer's measurement uncertainty is included in the 3.5% value of scatter and other effects, but just how much cannot be stated at this time. Although a value of 6% was assigned as an estimate of overall uncertainty surrounding the entire measurement process, it should be emphasized that the accelerometer's contribution is a fraction of the 6% under the conditions that these data were obtained.

4. CONCLUSIONS

Three of the more important transducer parameters were tested to obtain a measure of performance and to fundamentally characterize the accelerometer. These parameters were:

(1) Angular acceleration sensitivity as a function of frequency,

(2) Angular acceleration amplitude linearity, and

(3) Linear acceleration sensitivity response.

The angular acceleration sensitivity was measured over a frequency range from about 1.5 to 100 Hz and an acceleration amplitude range from about 64 to 5000 rad/s^2. The mean sensitivity as described in this report was 5.53 $\mu V \cdot s^2$/rad at a reference frequency of 15 Hz. Deviations of the sensitivity with frequency over a range from 1.5 to 70 Hz was about -1.5 to +2.5% referenced to the 15-Hz mean value.

The angular acceleration amplitude linearity was measured over an acceleration range from about 64 to 5000 rad/s^2. The maximum deviation between the measured data and a zero-based, best-fit, straight line was about -1.27%, a moderate portion of which can be attributed to uncertainties in making the measurement and analyzing the data.

The linear acceleration sensitivity was measured both parallel to and perpendicular to the angular sensing axis. In the first instance, measurements indicated performance was within the preliminary specifications as given by the manufacturer. In the second instance, the measurement is much more difficult and rocking motions of the vibration exciter (i.e., angular accelerations) contaminate the data so that good measurements could not be achieved. However, the results were well within an order of magnitude of being within the preliminary specifications and are small, even though a good measure could not be done.

Overall, based on the limited measurement results obtained and from the observed performance, it is felt that the quality is probably adequate for the current DoT application of measuring angular head motions. However, the accelerometer packaging configuration must be changed and adapted to the DoT application which would then require additional testing to ensure that the transducer performance was maintained.

Future testing should be done at a greater depth (i.e., more thoroughly), other parameters tested, and an attempt made to reduce the overall measurement uncertainties.

5. ACKNOWLEDGMENTS

Appreciation is given to Mark Haffner, the DoT/NHTSA technical contract monitor, for his support and guidance concerning the ultimate application for the type accelerometer and also for his probing questions regarding transducer operation and testing methodology. Thanks are extended to Bob Sill of Endevco regarding details of the accelerometer design and construction as well as interpretation of some of the specifications. Thanks also to several NBS co-workers who contributed suggestions.

6. REFERENCES

[1] Endevco angular accelerometer, model 7302, serial no. 102 prototype.

[2] Personal communication with R. Sill of Endevco, October 14, 1980.

[3] Harris, C. M., Crede, C. E., "Shock and Vibration Handbook," Second Edition, McGraw-Hill, New York, 1976, p. 2-9.

[4] Personal communication with R. Sill of Endevco, November 17, 1980.

[5] Ramboz, J. D., Angular Acceleration Generation Using a Dual Spin-Axis Rate-Table. Nat. Bur. Stand. (U.S.) NBSIR 81-xxxx, being prepared.

[6] McCuskey, S. W., "Introduction to Advanced Dynamics," Addison-Wesley, Reading, Mass., 1959, pp. 120-124.

[7] "Handbook of Instructions, 1100 series, Rate Tables," Genisco Technology Corporation, Compton, Calif., June 1, 1973.

Table 1 - Transducer gage resistance measurements; values are in units of kilohms.

		Red meter lead				
		+INPUT	-INPUT	+OUTPUT	-OUTPUT	SHIELD
Black meter lead	+INPUT	--	1.66	1.32	1.27	00
	-INPUT	1.67	--	1.26	1.21	00
	+OUTPUT	1.32	1.26	--	1.66	00
	-OUTPUT	1.27	1.21	1.66	--	00
	SHIELD	00	00	00	00	--

Table 2 - Angular velocities ν_1 and ν_2 for calculated peak acceleration, α

	Upper Platform Velocity	Main Platform Angular Velocity ν_1, °/s											
		Angular acceleration amplitude, rad/s^2 peak											
Test Freq Hz	ν_2 rpm	50	100	250	500	1000	2000	3000	4000	5000	6000	7000	7896
1.67	100		54.7	1368	2736	--	--	--	--	--	--	--	--
3	180			760	1520	3040	--	--	--	--	--	--	--
5	300			456	912	1824	--	--	--	--	--	--	--
7	420			326	651	1303	2605	--	--	--	--	--	--
10	600	45.6	91.2	228	456	912	1824	2736	--	--	--	--	--
15	900	30.4	60.8	152	304	608	1216	1824	2432	3040	--	--	--
30	1800			76.0	152	304	608	912	1216	1520	1824	2128	2400
50	3000			45.6	91.2	182	365	547	730	912	1094	1277	1440
70	4200			32.6	65.1	130	261	391	521	651	782	912	1029
100	6000			22.8	45.6	91.2	182	274	365	456	547	638	720

rpm x $\pi/30$ = rad/s

°/s x $\pi/180$ = rad/s

Table 3 - Measured gains and gain slope corrections for the cascaded filters and amplifiers used for the angular acceleration sensitivity measurements. (LP = low pass, HP = high pass)

Nominal Frequency Hz	Nominal Gain	Measured Gain	Gain Slope %/Hz	Filter Settings		
				Preamp. Hz	Filter A Hz	Filter B Hz
1.5	500	500.00	0.00	.03HP/30LP	15LP	15LP
2	500	413.87	-1.64	.03HP/3LP	4LP	4LP
3	500	498.75	-0.201	.03HP/30LP	15LP	15LP
3	200	199.32	-0.401	.03HP/30LP	15LP	15LP
5	500	493.91	-0.640	.03HP/30P	15LP	15LP
7	500	484.49	-1.064	.03HP/30LP	15LP	15LP
10	500	498.50	-0.149	.03HP/100LP	30LP	30LP
15	500	491.88	-0.439	.03HP/100LP	30LP	30LP
15	500	479.24	+0.144	3HP/100LP	30LP	30LP
15	200	196.62	-0.432	.03HP/100LP	30LP	30LP
15	200	190.49	+0.467	3HP/100LP	30LP	30LP
30	500	474.84	-0.496	3HP/100LP	55LP	55LP
30	200	188.14	-0.545	3HP/100LP	55LP	55LP
70	500	379.35	+2.714	3HP/300LP	60HP	60HP
70	500	428.63	+2.056	3HP/300LP	60HP	150LP
70	200	171.17	+2.89	3HP/300LP	60HP	150LP
100	500	449.68	-0.698	3HP/300LP	65HP	150LP

Table 4 - Amplitude linearity data over 10 percent of the acceleration full-scale range of 50 000 rad/s^2. Reference sensitivity was 5.53 μV·s^2/rad; % deviation is deviation between fit value and measured value

Acceleration rad/s^2	Meas. Sensitivity μV · s^2/rad	% Deviation
64	5.486	-0.80
100	5.472	-1.05
250	5.503	-0.49
500	5.46	-1.27
1000	5.531	+0.02
2000	5.498	-0.58
3000	5.567	+0.67
4000	5.575	+0.81
5000	5.573	+0.78

Table 5 - Linear acceleration sensitivity parallel to the angular acceleration sensitive axis

Frequency Hz	Linear Sensitivity $rad/s^2 \cdot g$	Preliminary Spec. $rad/s^2 \cdot g$
24.5	0.66	2.5
50	0.80	2.5
100	2.10	5.0
150	4.2	7.5
200	8.4	10.0
250	3.0	12.5
300	12.6	15.0
350	17.5	17.5
400	22.8[a]	20.0
500	29.0[a]	25.0
600	37.4[a]	30.0
700	45.0[a]	35.0

[a]This value contains angular acceleration components due to the rocking motion of the vibrator exciter and is therefore greater than the "pure linear response." The exact amount is unknown, but shown to indicate a trend in the linear acceleration response with frequency.

Table 6 - Linear acceleration sensitivity perpendicular to the angular acceleration sensitive axis for two positions; see text for explanation

Frequency Hz	Linear Sensitivity[c], rad/s^2·g·Hz	
	Position 1	Position 2
100	0.180	0.089
150	0.112	0.055
200	0.121	0.059
250	0.109	0.054
300	0.180	0.090
350	0.199	0.100
400	0.204	0.102
500	0.149	0.075
600	0.186[b]	---
700	0.277[a,b]	---

[a] Gain, H, was set to 500 rather than 1000.

[b] Harmonic distortion present in waveform.

[c] Values shown also have a vector component included due to rocking motion (i.e., exciter angular acceleration) causing values to be larger than the true linear response.

Table 7 - Results of the analysis for an estimate of standard deviation calculated from 229 data sets. See figure 18 for a plot of the data

Freq., Hz	No. of Meas.	Estimated % Std. Dev.
1	9	1.1
3	9	1.5
5	15	1.0
7	18	3.3
10	21	3.2
15	42	1.3
30	29	1.0
70	62	3.2
100	24	3.1

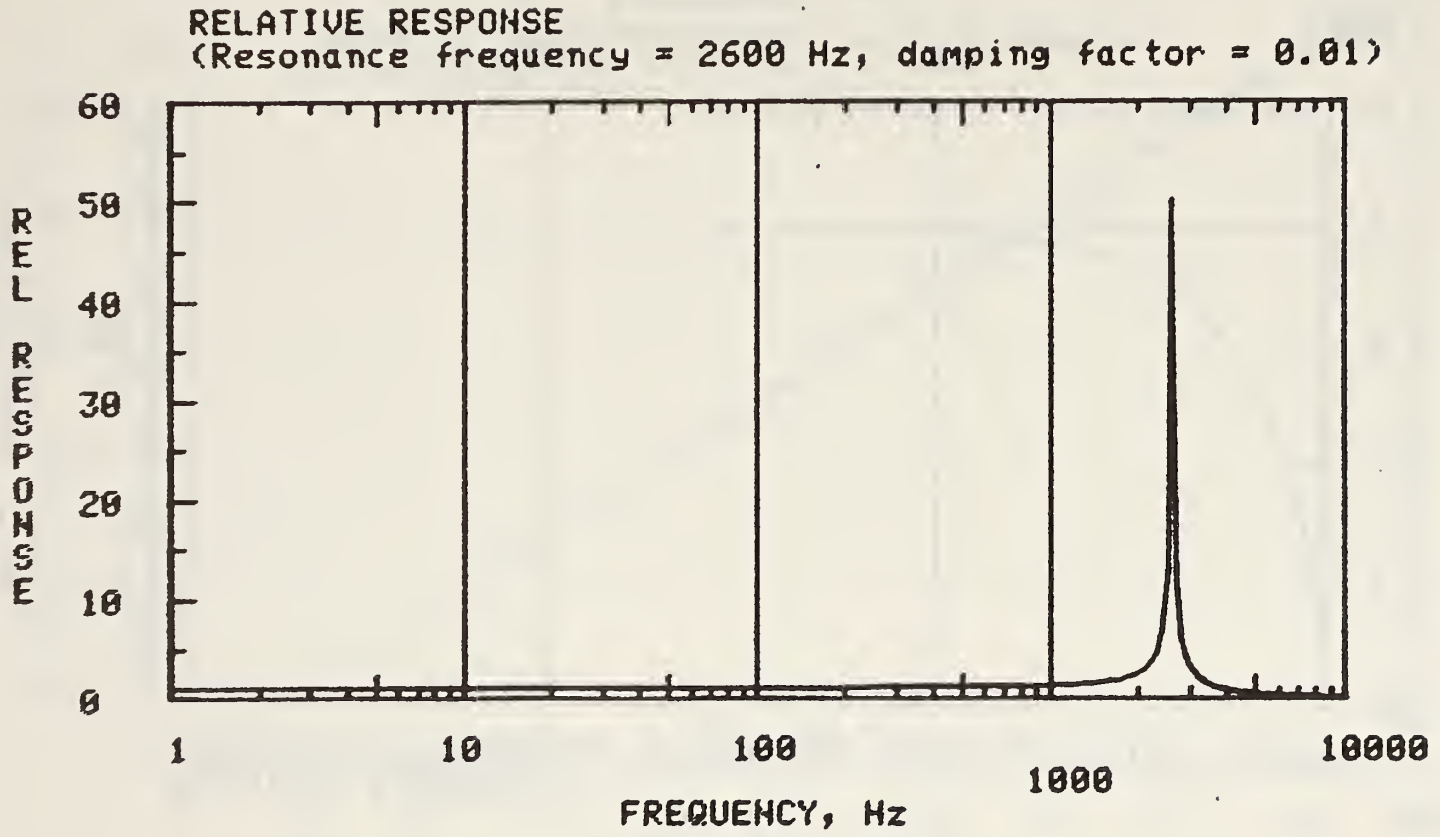

Figure 1A. Theoretical frequency response for an angular accelerometer having a resonance frequency of 2600 Hz and a damping factor of 0.01.

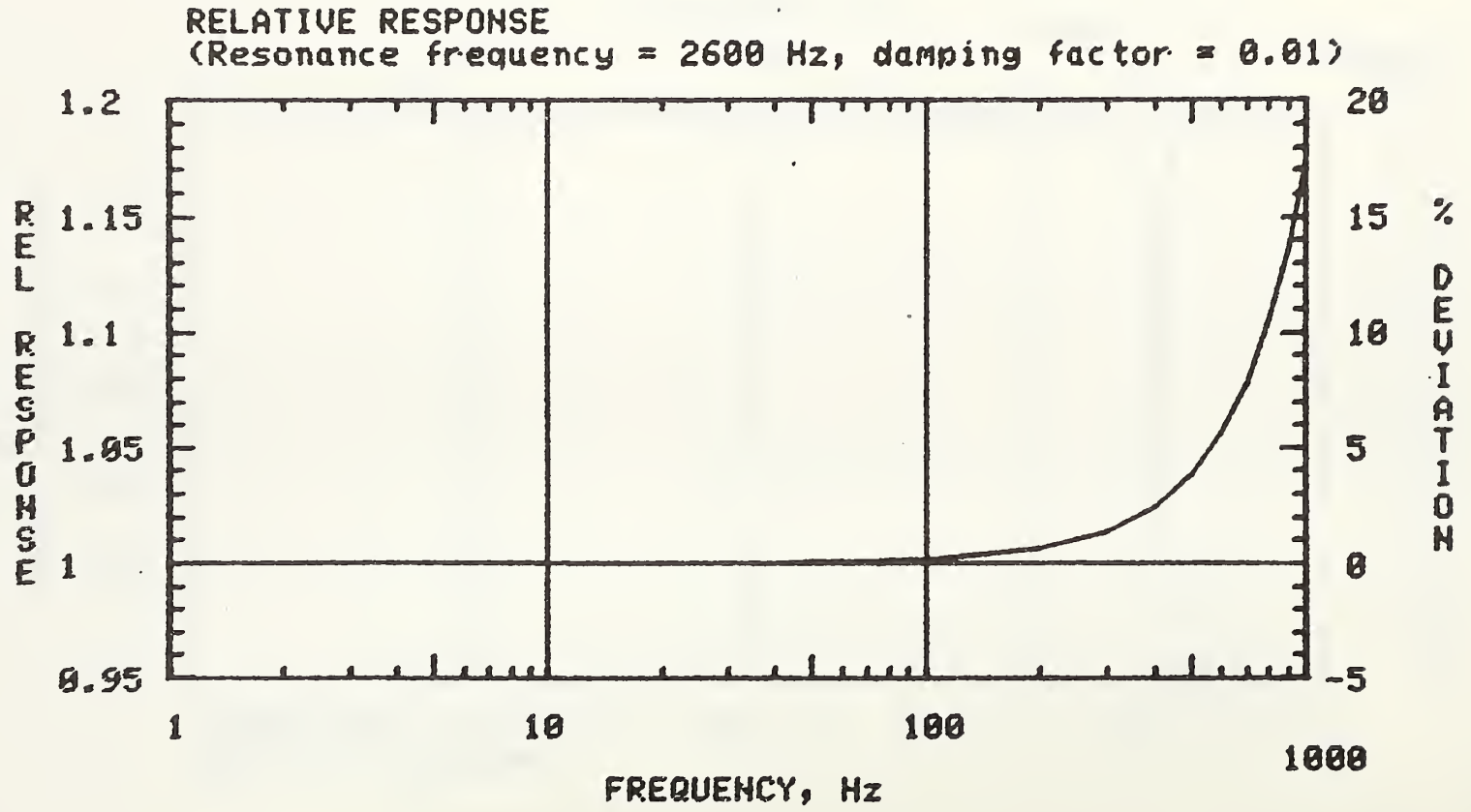

Figure 1B. Theoretical frequency response same as Fig. 1A except shown over compressed frequency and relative response ranges.

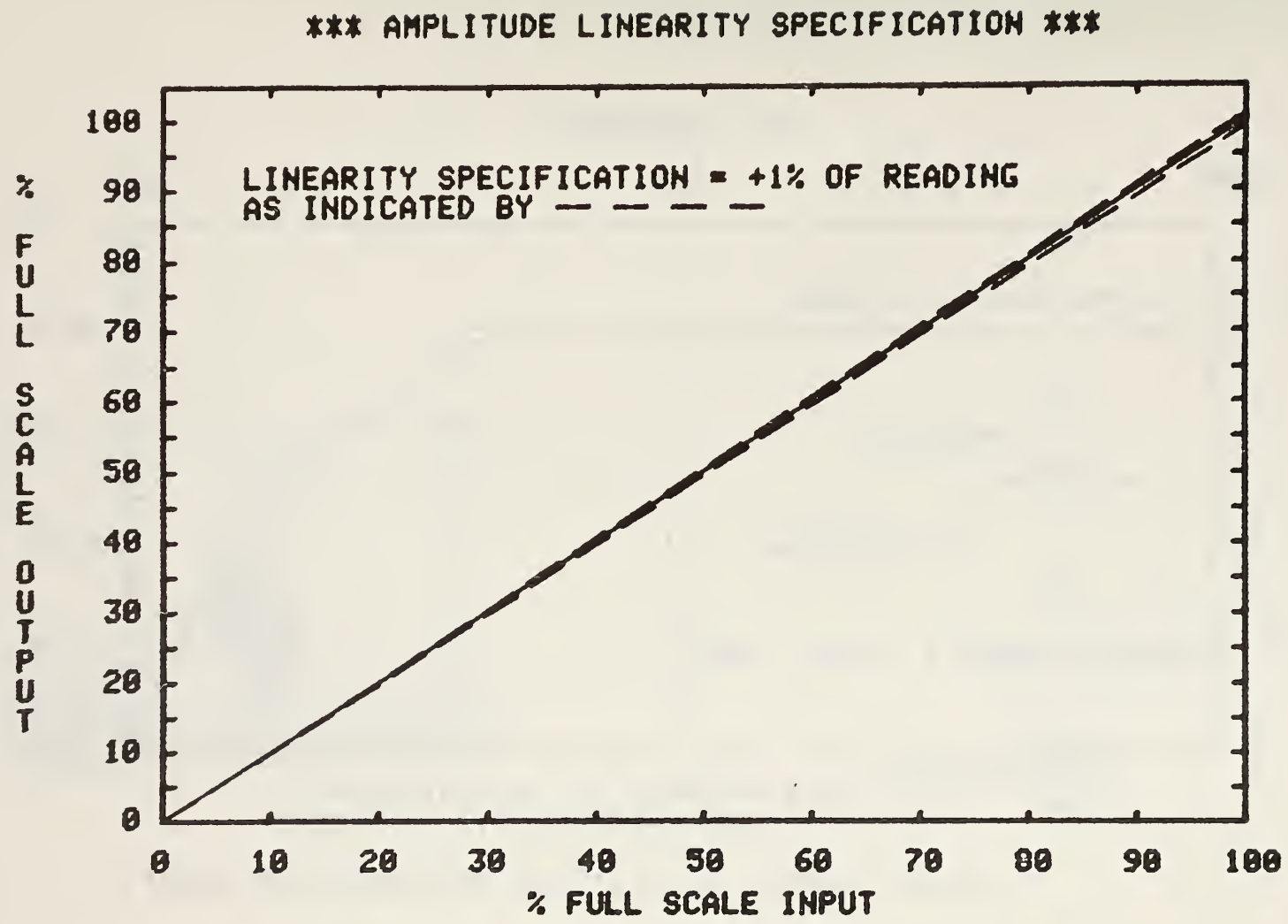

Figure 2. Angular acceleration amplitude linearity preliminary specification.

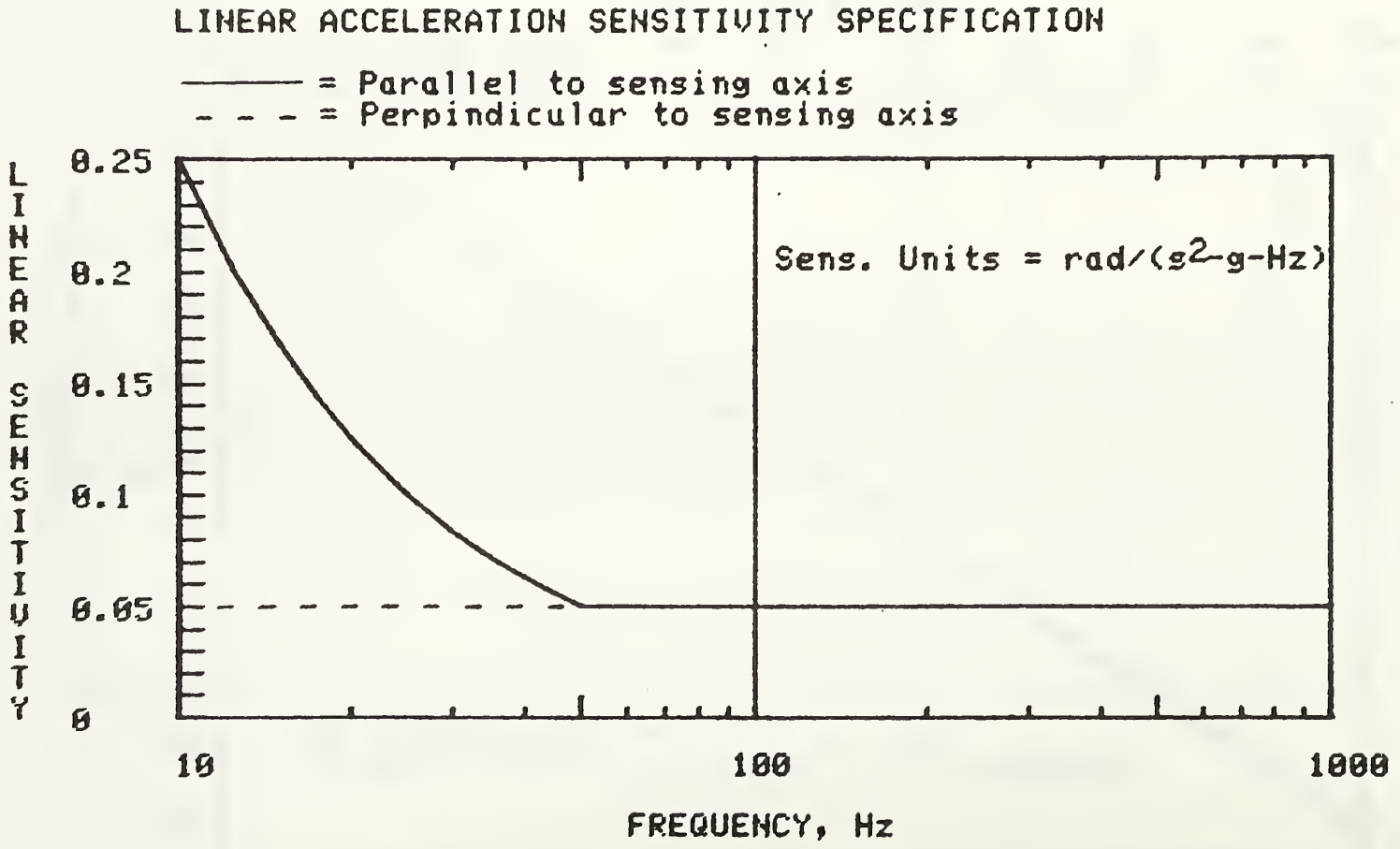

Figure 3. Transducer sensitivity to linear acceleration input both parallel and perpendicular to the sensing axis.

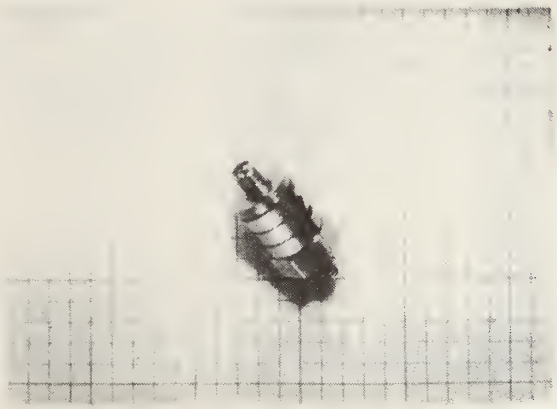

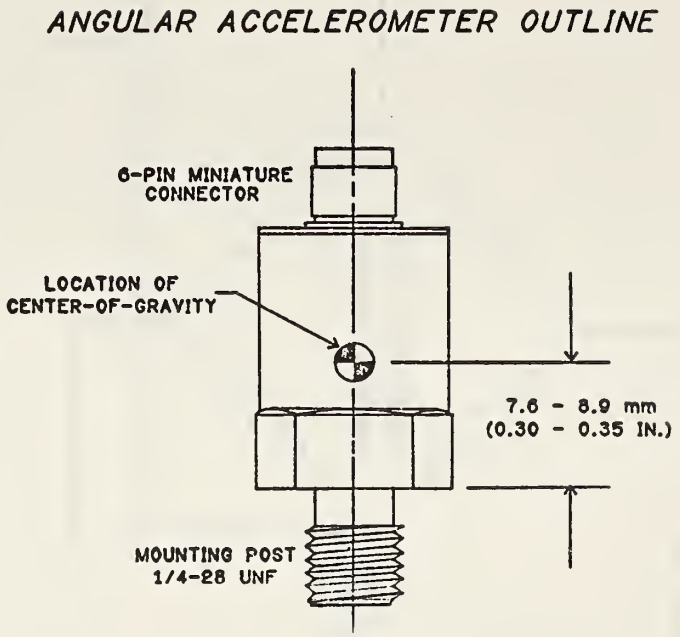

Figure 4. Photograph and outline of angular accelerometer.

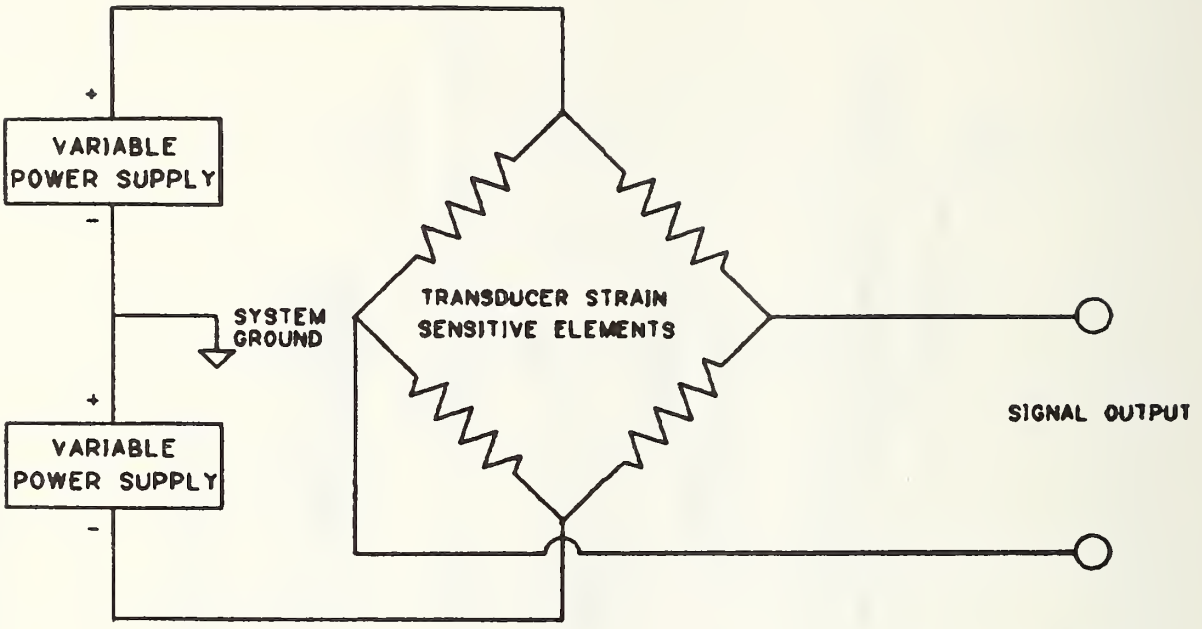

Figure 5. Transducer bridge elements and split power supplies to force output residual voltage to near zero volts.

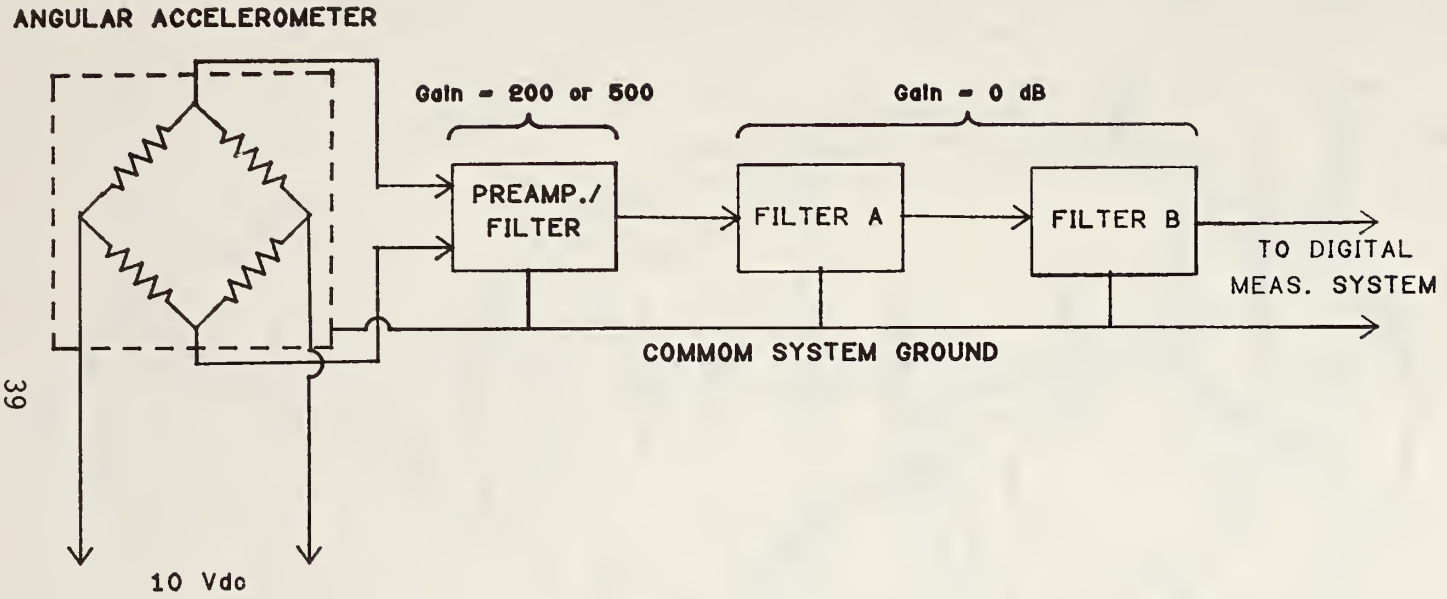

Figure 6. Accelerometer, amplifiers, and filters block diagram.

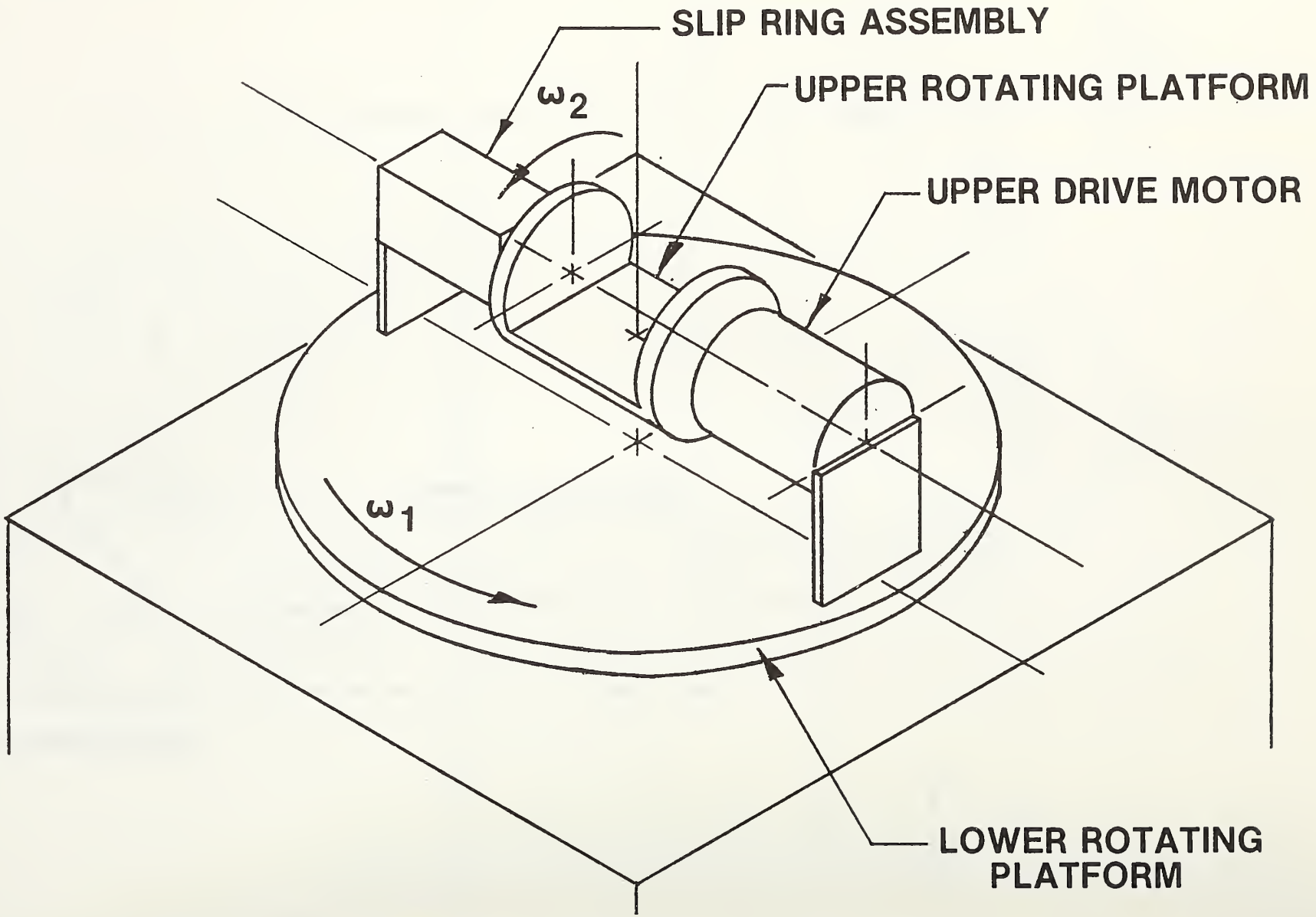

Figure 7. Basic elements of the dual spin-axis rate-table (DSART). Angular accelerometer to be calibrated is mounted on the upper rotating platform.

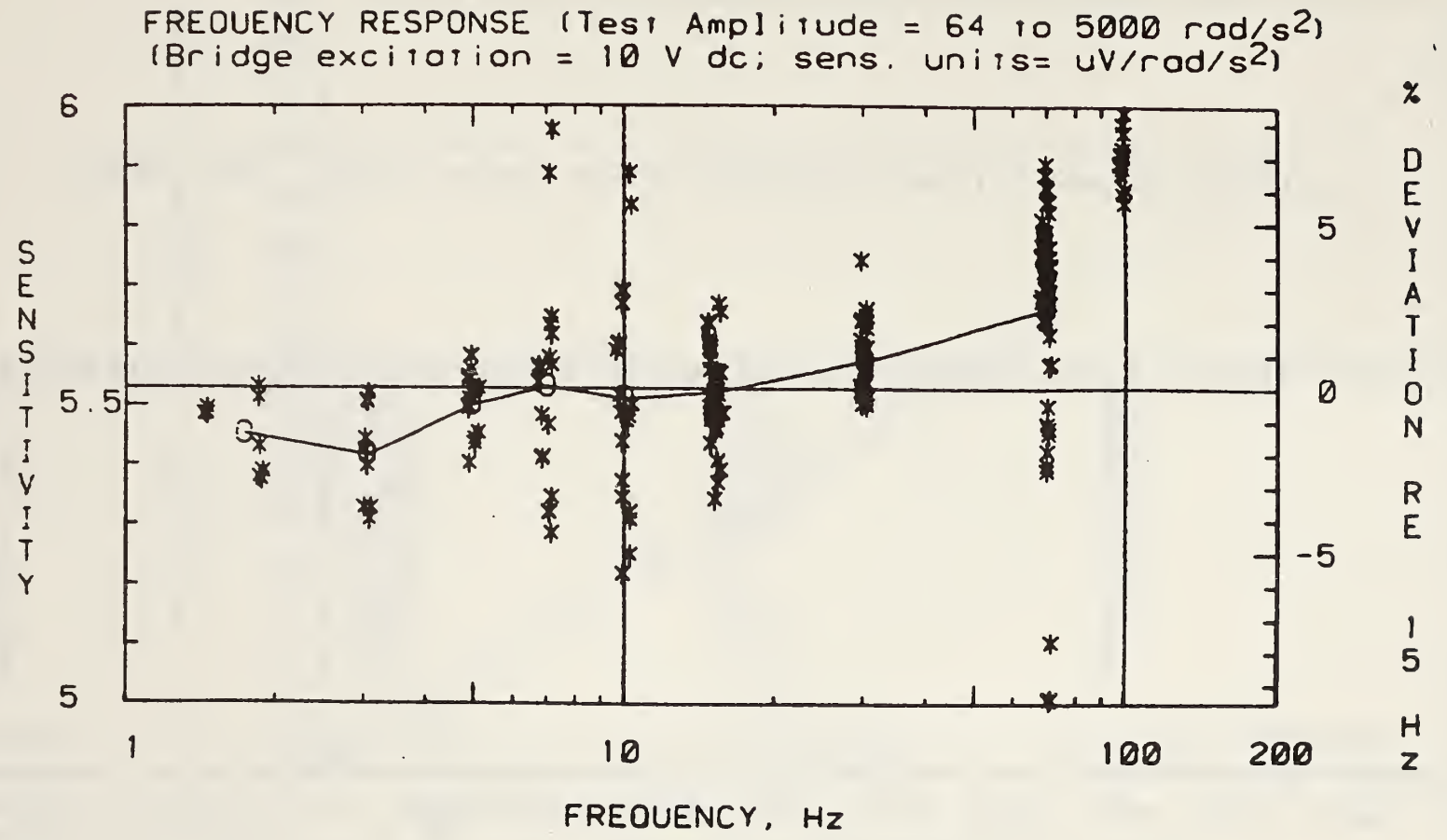

Figure 8A. Angular acceleration measurement results summary; sensitivity vs. frequency at acceleration from 64 to 5000 rad/s^2.

09-DEC-80 08:45:05

****

TAPE FILE: 36

ACCELERATION AMPLITUDE: 0 rad/s^2

REFERENCE FREQUENCY: 15 Hz

REFERENCE SENSITIVITY: 5.529 uV/rad/s^2

****

FREQUENCY	SENSITIVITY	% DEVIATION	No. of READINGS
1.73	5.451	-1.5	9
3.08	5.416	-2.1	9
5.01	5.501	-0.6	15
7.08	5.533	0	18
10.1	5.512	-0.4	21
15.25	5.523	-0.2	42
30.38	5.575	0.8	29
70.2	5.663	2.4	62
99.93	6.04	9.2	24

****

Figure 8B. Angular acceleration measurement results summary; sensitivity vs. frequency at acceleration from 64 to 5000 rad/s^2.

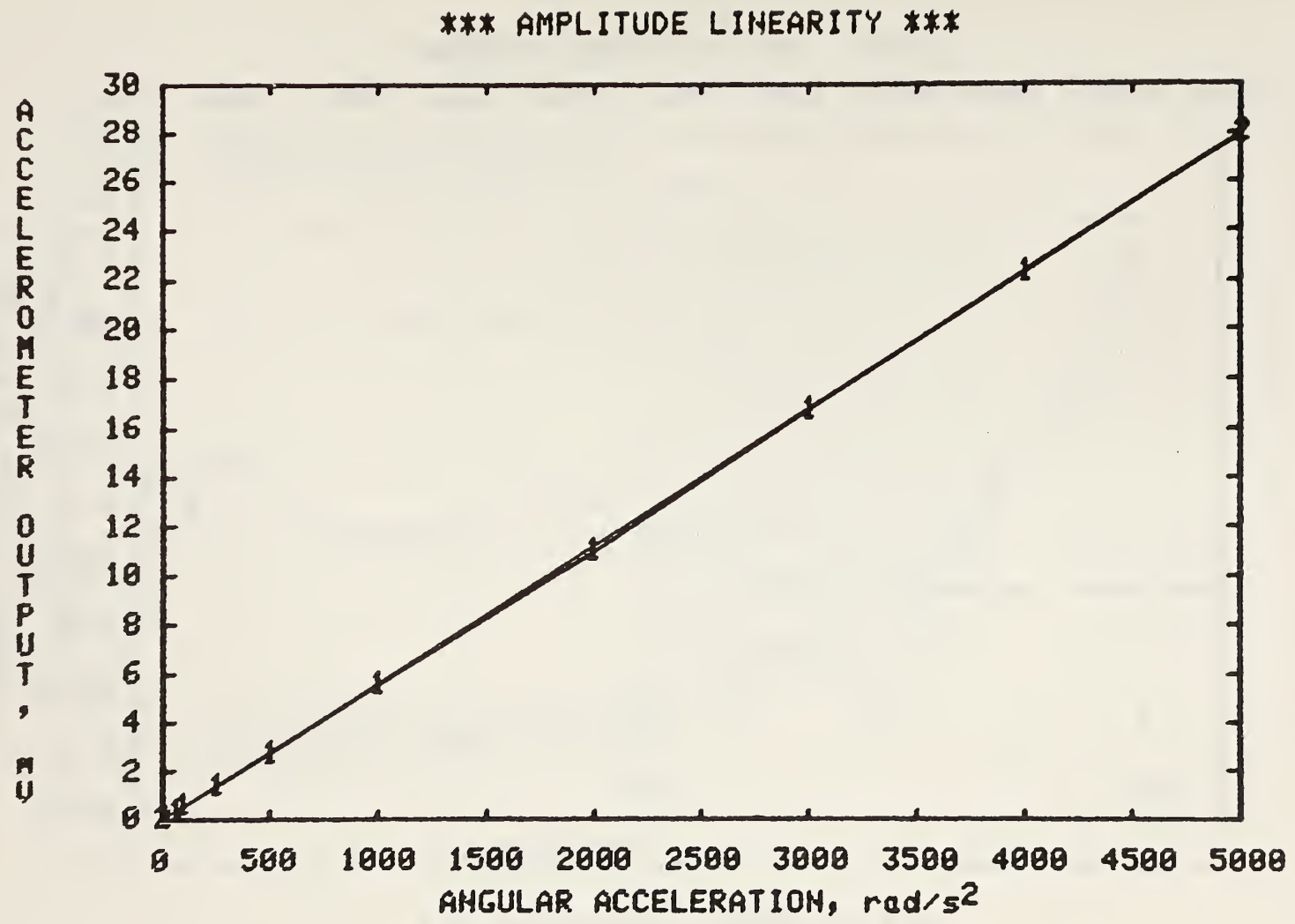

Figure 9. Angular acceleration measurement data results for the amplitude linearity; accelerometer output vs. acceleration. Note straight line also plotted.

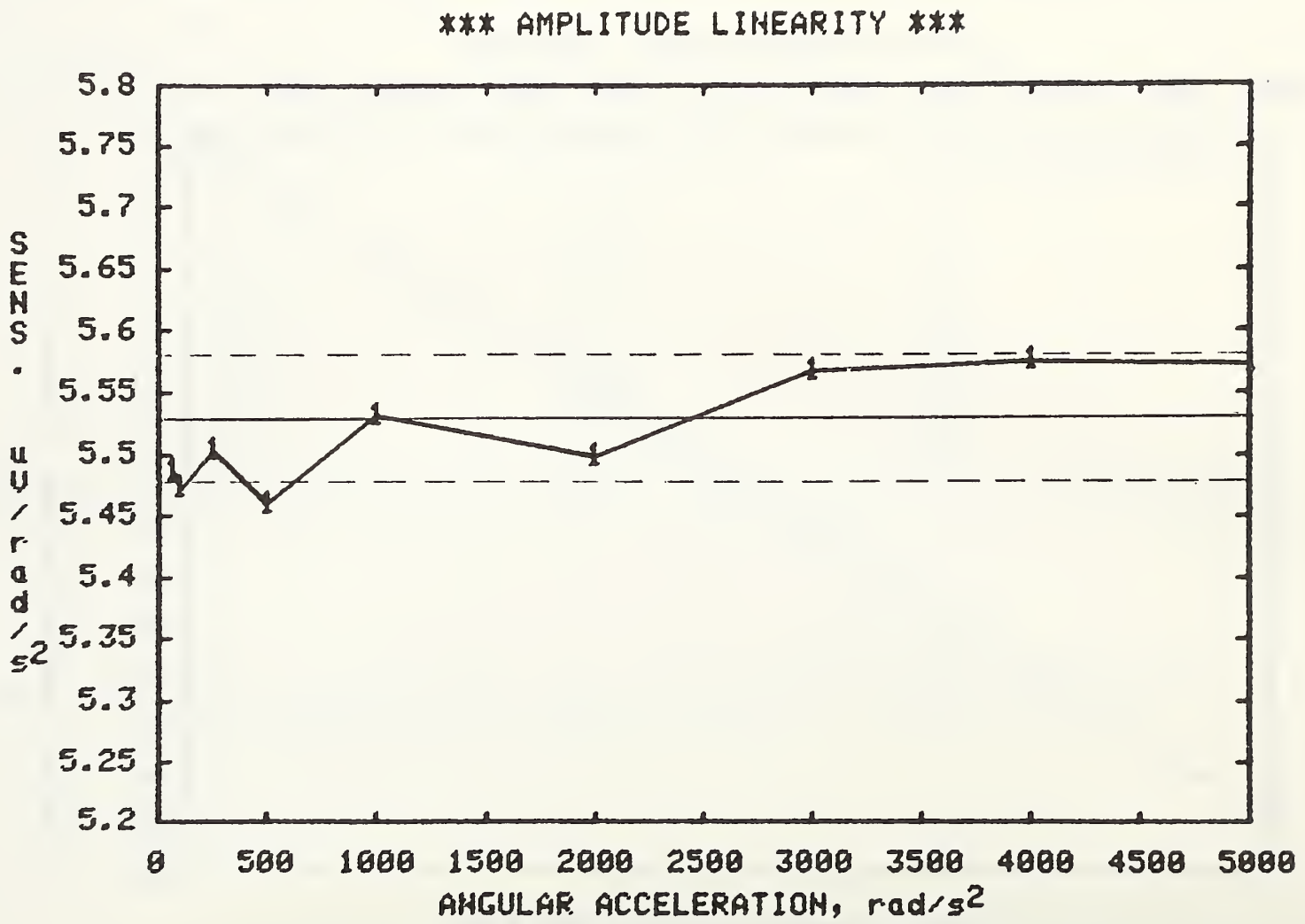

Figure 10. Angular acceleration data for amplitude linearity; transducer sensitivity vs. acceleration.

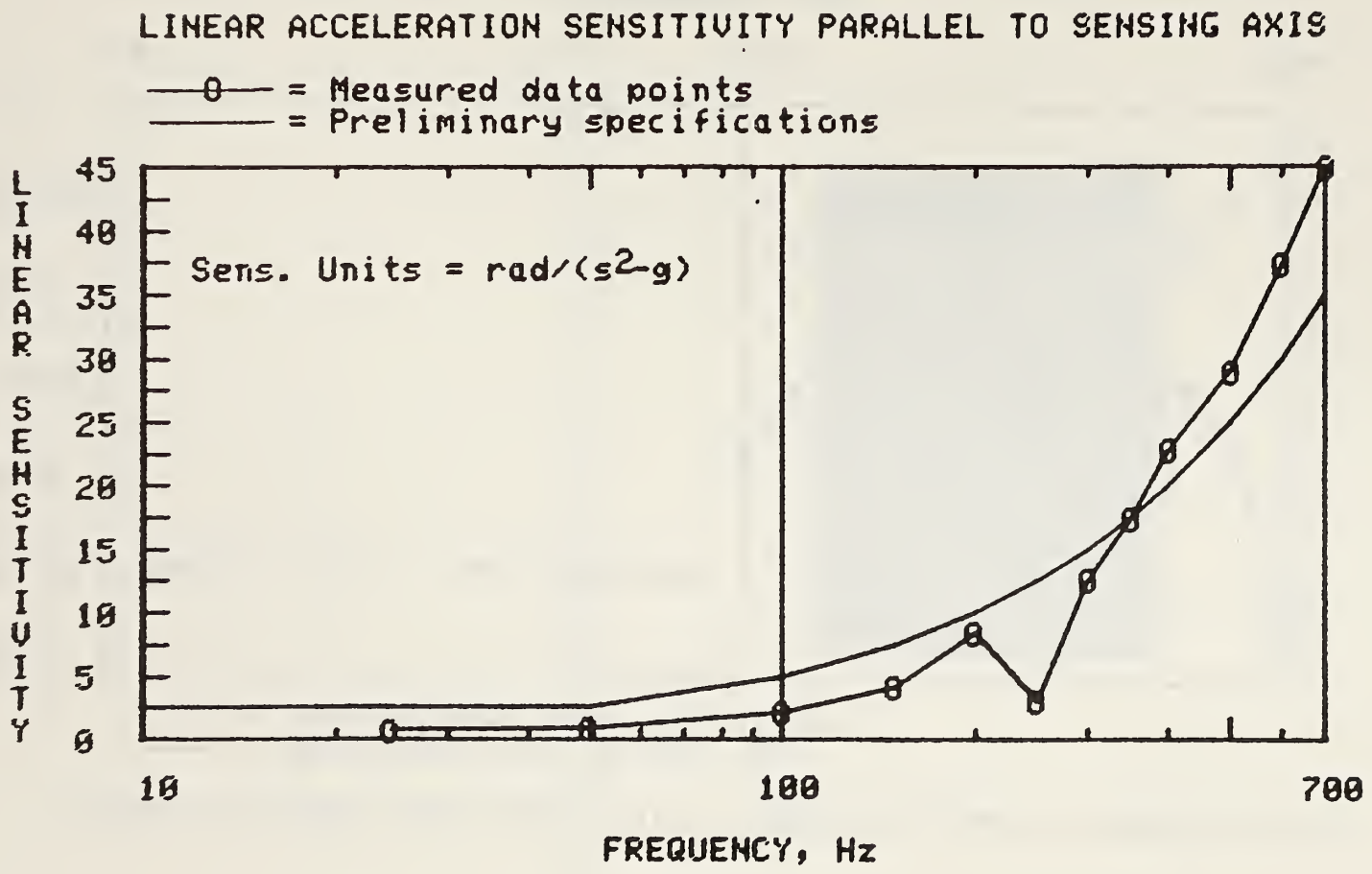

Figure 11. Linear acceleration sensitivity parallel to the angular sensitivity axis.

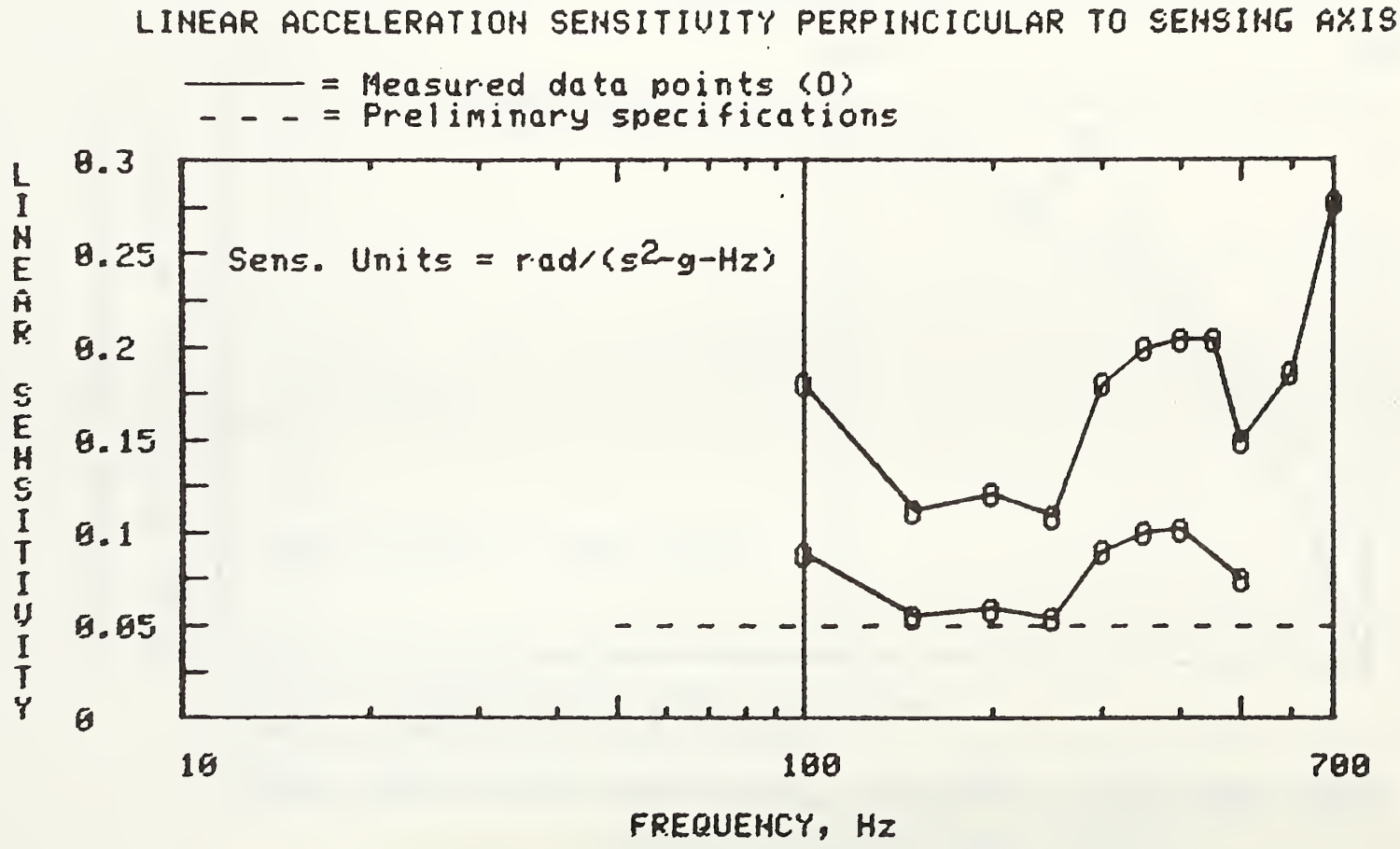

Figure 12. Linear acceleration sensitivity measurement results perpendicular to the angular sensitivity axis. Data shown for two orientations of the accelerometer about its sensing axis. Results are approximate and are "contaminated" with rocking motion of the exciter.

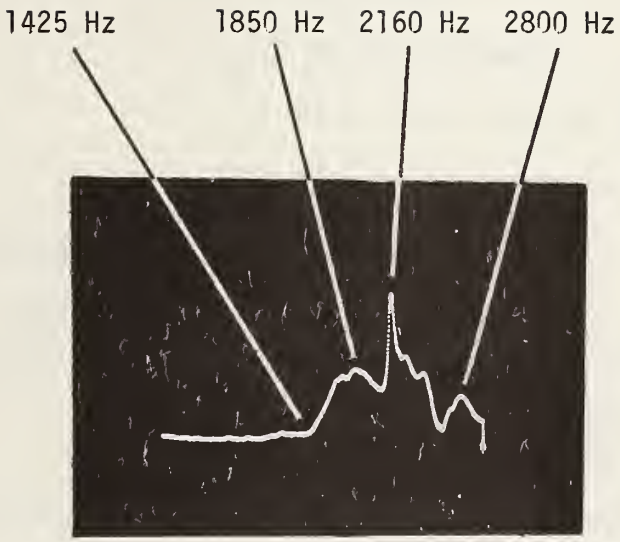

Figure 13. Resonant response of the accelerometer when excited by linear acceleration perpendicular to the angular sensing axis.

APPENDIX A

Preliminary Specification

7302 Angular Accelerometer S/N 102

Sensitivity	5.7 $\mu V\text{-}sec^2$/radian with 10 V excitation
Full Scale	50 000 rad/sec^2
Frequency Response	Flat within 1 dB to approximately 700 Hz
Phase Response	Typical of undamped system
Mounted Resonant Frequency	2600 Hz
Linear Acceleration Sensitivity	
Parallel to mounting surface:	Increases directly with frequency $0.04 \text{ to } 0.05 \frac{rad}{sec^2 - G - Hz}$
Parallel to transducer axis:	2.5 rad/sec^2 - G from dc to $\approx$ 50 Hz, increasing directly with frequency above $\approx$ 50 Hz at about 0.05 rad/sec^2 - G - Hz
Transverse Axis Angular Sensitivity	3% maximum, 2% typical
Shock Limits	
Angular	$\approx$ 500,000 rad/sec^2
Linear	$\approx$ 5000 G's
Amplitude Linearity	Less than 1% nonlinearity
Temperature	+10% at 25°F -15% at 175°F
Physical Description	15 grams, 3 cm long, stainless steel case with 1/2" hex faces, 1/4 x 28 mounting post
Electrical Connection	Six-pin receptacle
Maximum Mounting Torque	One foot-pound

APPENDIX B

FREQUENCY RESPONSE MEASUREMENT DATA

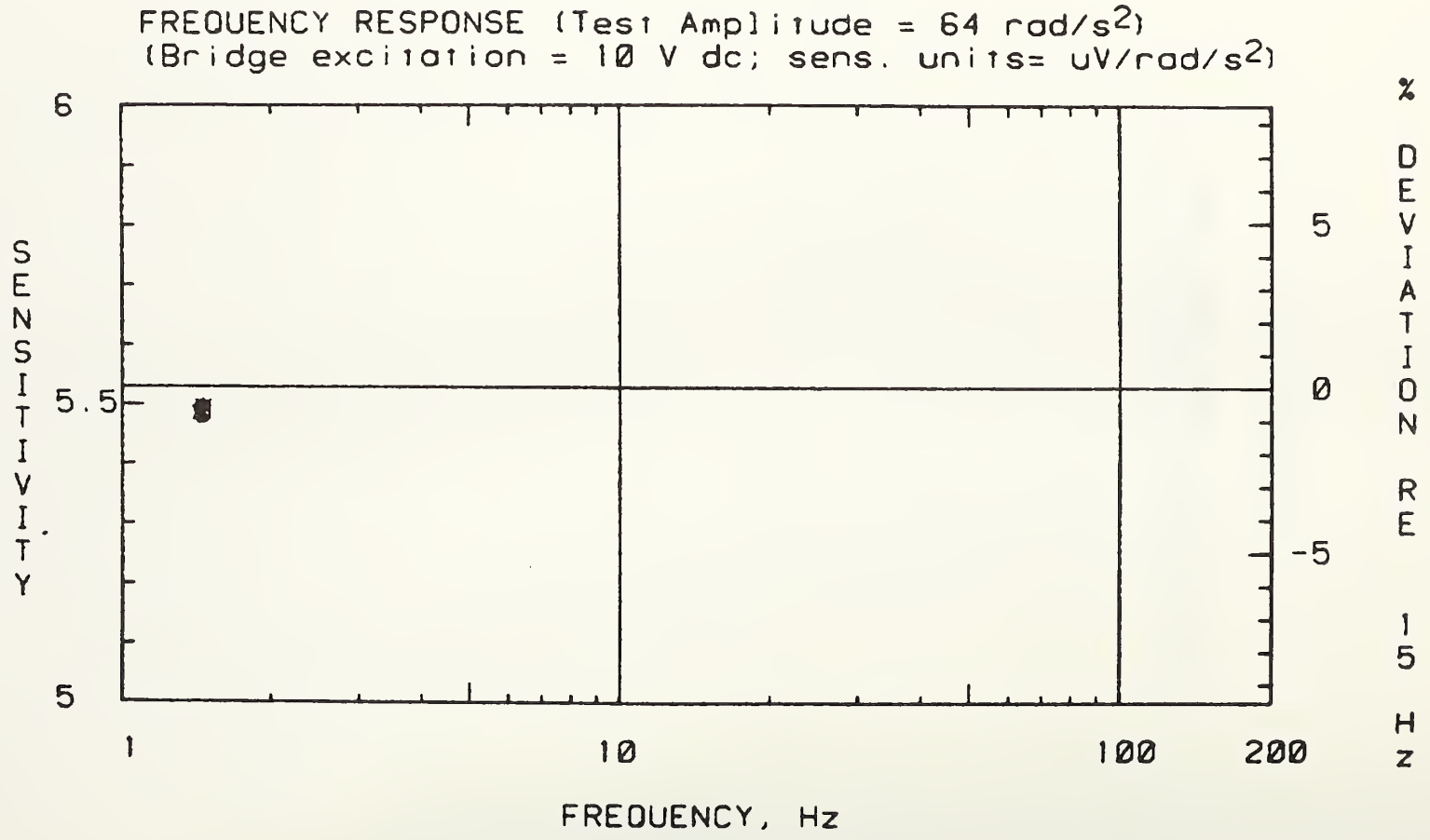

Figure B-1A. Angular acceleration measurement results; sensitivity vs. frequency at an acceleration of 64 rad/s^2.

08-DEC-80 09:33:18

****

TAPE FILE: 23

ACCELERATION AMPLITUDE: 64 rad/s^2

REFERENCE FREQUENCY: 15 Hz

REFERENCE SENSITIVITY: 5.529 uV/rad/s^2

****

FREQUENCY	SENSITIVITY	% DEVIATION	No. of READINGS
1.46	5.486	-0.8	3

****

Figure B-1B. Angular acceleration measurement results; sensitivity vs. frequency at an acceleration of 64 rad/s^2.

08-DEC-80 09:39:35

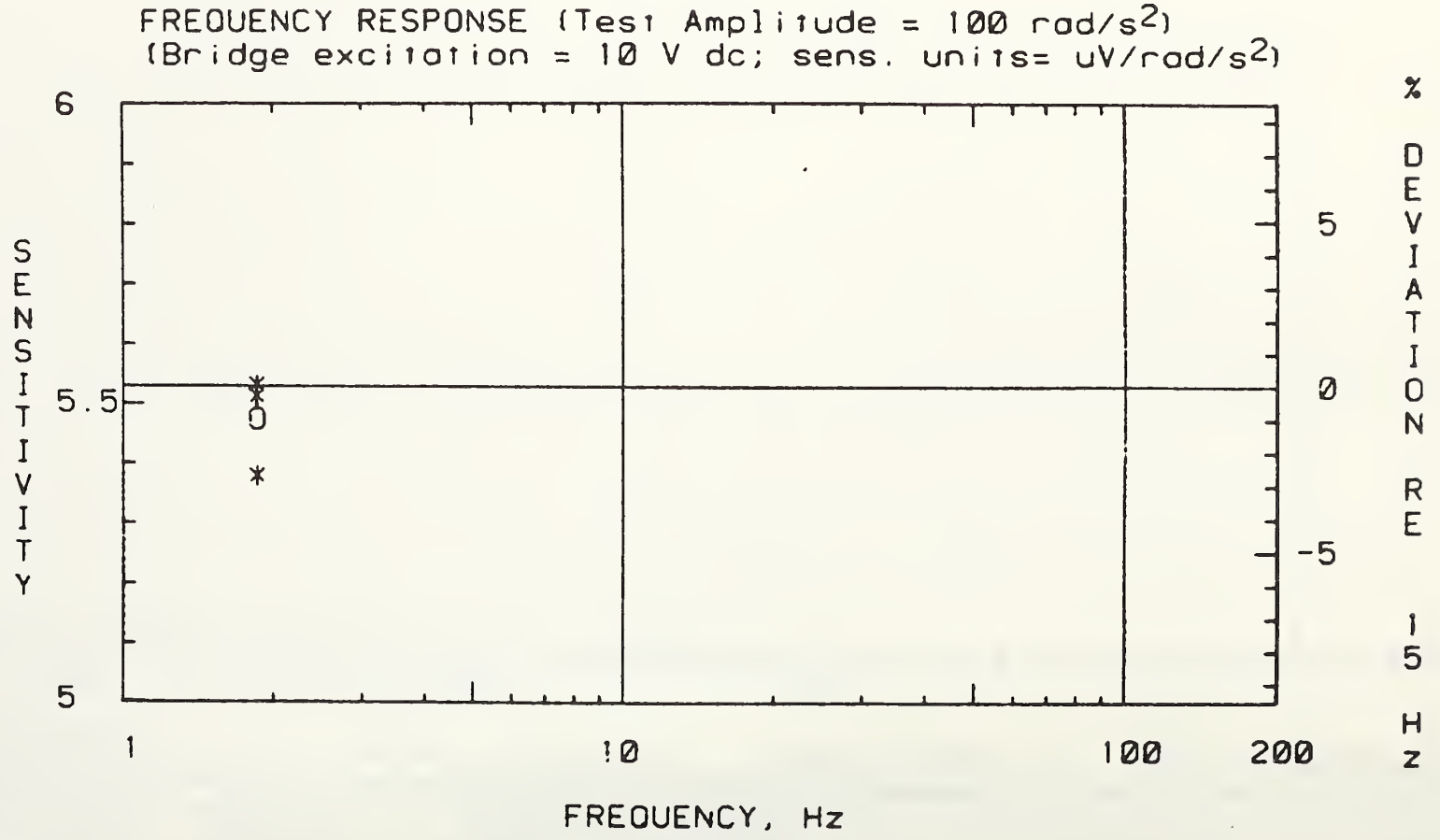

Figure B-2A. Angular acceleration measurement results; sensitivity vs. frequency at an acceleration of 100 rad/s^2.

08-DEC-80 09:40:08

****

TAPE FILE: 33

ACCELERATION AMPLITUDE: 100 rad/s^2

REFERENCE FREQUENCY: 15 Hz

REFERENCE SENSITIVITY: 5.529 uV/rad/s^2

****

FREQUENCY	SENSITIVITY	% DEVIATION	No. of READINGS
1.86	5.472	-1.1	3

****

Figure B-2B. Angular acceleration measurement results; sensitivity vs. frequency at an acceleration of 100 rad/s^2.

09-DEC-80 09:37:20

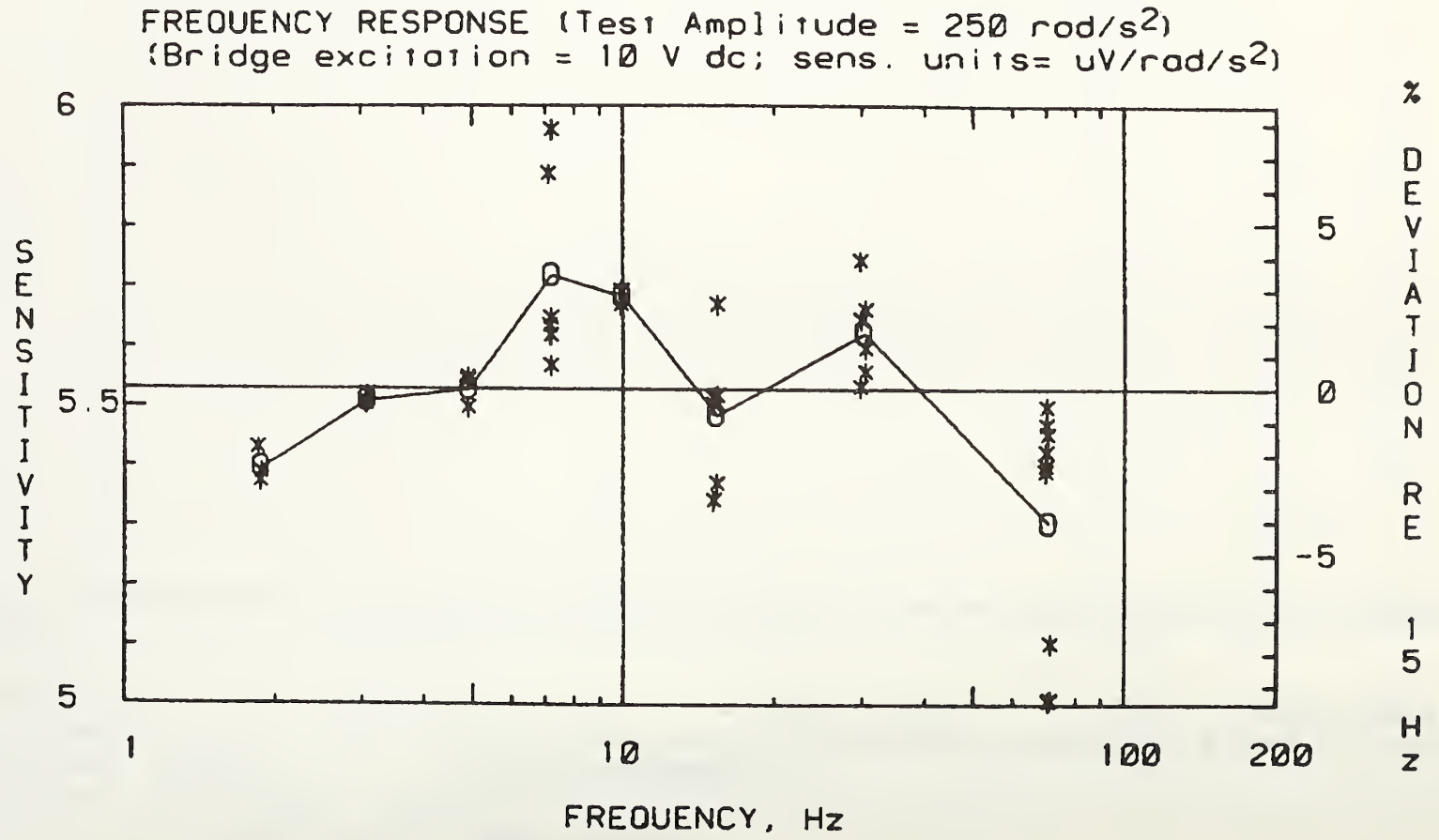

Figure B-3A. Angular acceleration measurement results; sensitivity vs. frequency at an acceleration of 250 rad/s^2.

09-DEC-80 09:38:18

****

TAPE FILE: 25

ACCELERATION AMPLITUDE: 250 rad/s^2

REFERENCE FREQUENCY: 15 Hz

REFERENCE SENSITIVITY: 5.529 uV/rad/s^2

****

FREQUENCY	SENSITIVITY	% DEVIATION	No. of READINGS
1.88	5.396	-2.5	3
3.08	5.509	-0.4	3
4.92	5.528	-0.1	3
7.22	5.718	3.4	6
10	5.683	2.7	3
15.4	5.485	-0.8	6
30.32	5.621	1.6	6
70.86	5.304	-4.1	9

****

Figure B-3B. Angular acceleration measurement results; sensitivity vs. frequency at an acceleration of 250 rad/s^2.

09-DEC-80 10:24:20

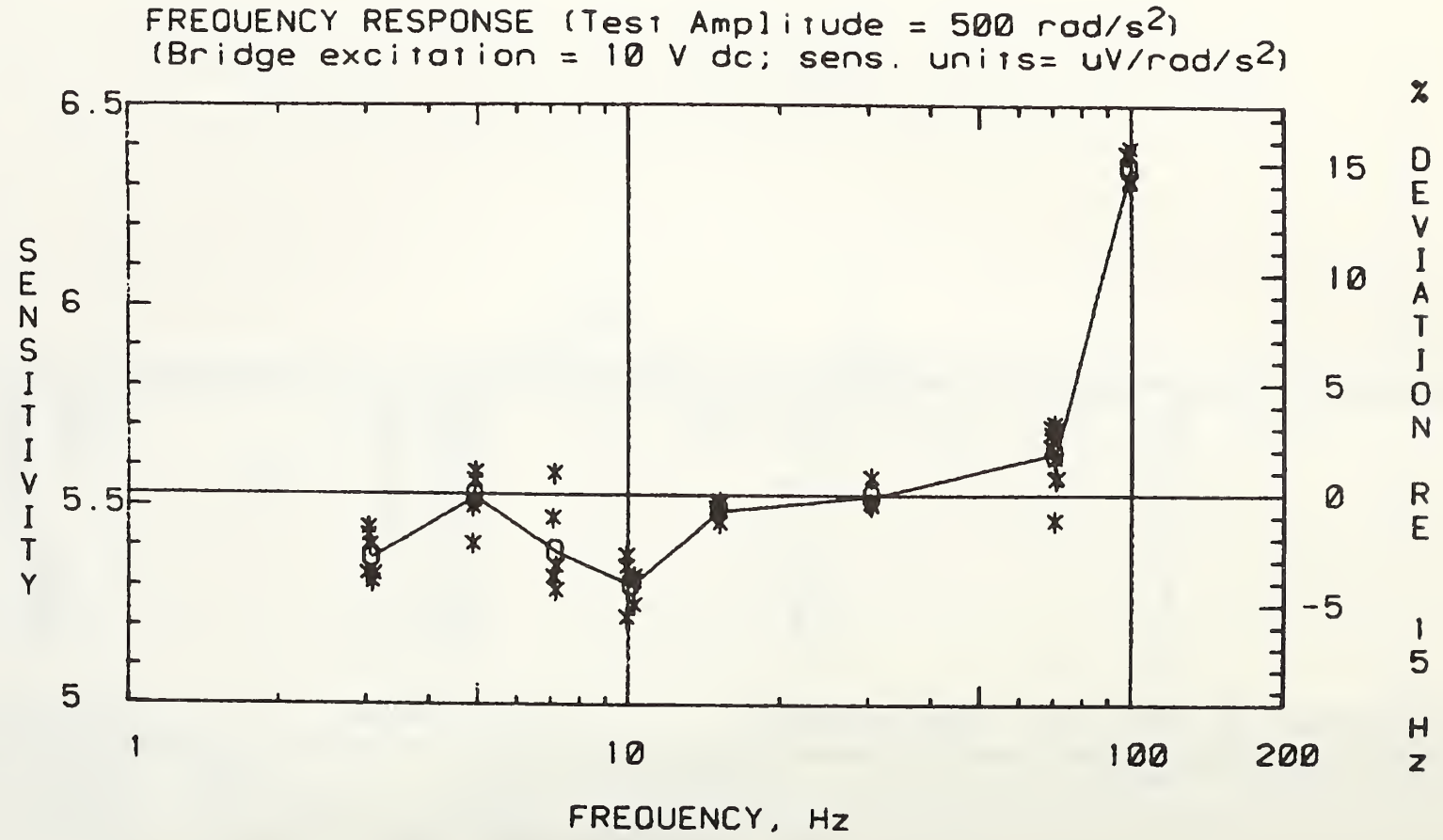

Figure B-4A. Angular acceleration measurement results; sensitivity vs. frequency at an acceleration of 500 rad/s^2.

09-DEC-80 10:24:35

****

TAPE FILE: 26

ACCELERATION AMPLITUDE: 500 rad/s^2

REFERENCE FREQUENCY: 15 Hz

REFERENCE SENSITIVITY: 5.529 uV/rad/s^2

****

FREQUENCY	SENSITIVITY	% DEVIATION	No. of READINGS
3.07	5.37	-2.9	6
4.96	5.52	-0.2	6
7.17	5.385	-2.7	6
10.17	5.302	-4.2	6
15.21	5.488	-0.8	6
30.61	5.524	-0.1	3
70.73	5.632	1.8	10
99.84	6.349	14.8	6

****

Figure B-4B. Angular acceleration measurement results; sensitivity vs. frequency at an acceleration of 500 rad/s^2.

09-DEC-80 10:27:18

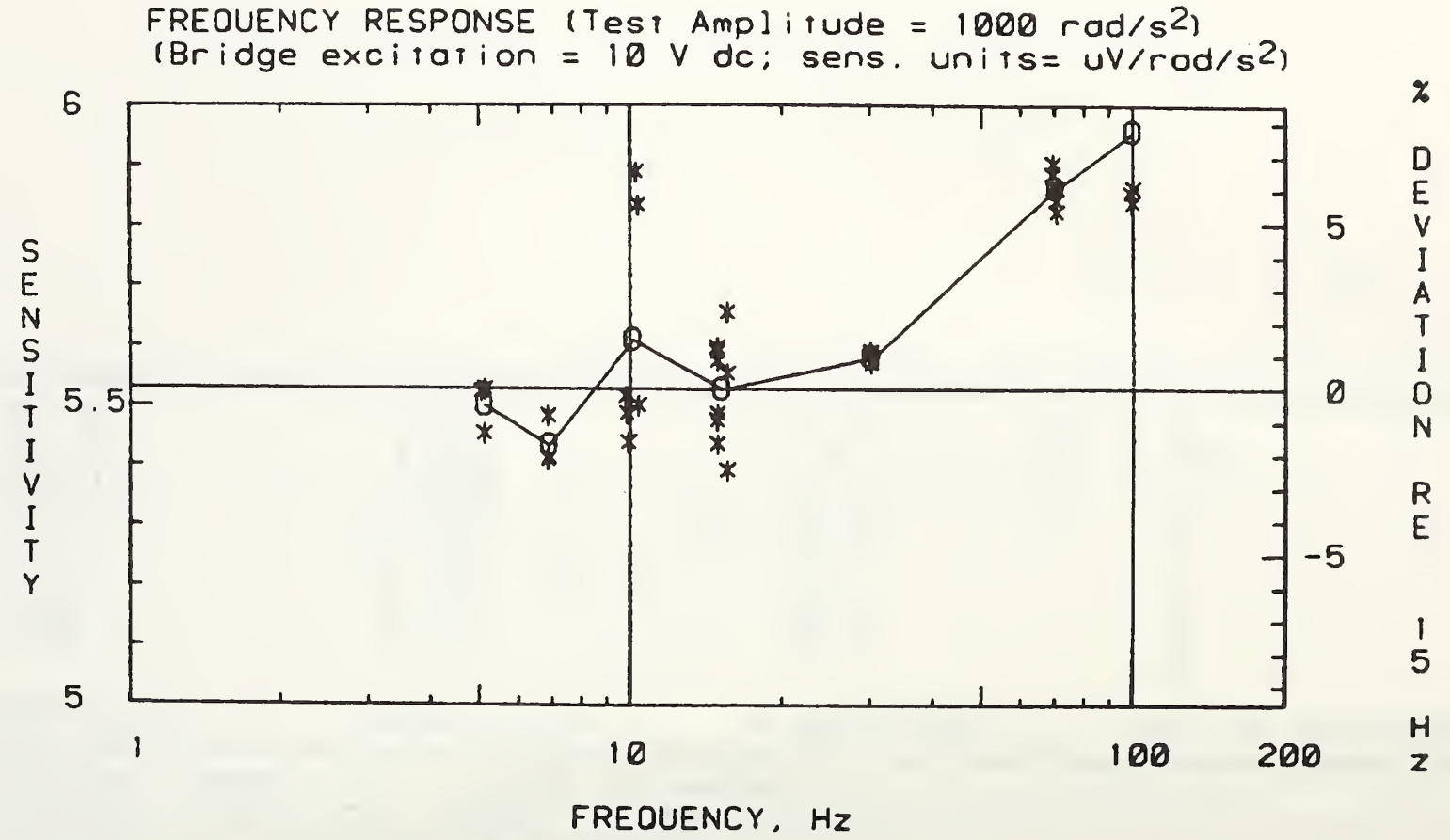

Figure B-5A. Angular acceleration measurement results; sensitivity vs. frequency at an acceleration of 1000 rad/s^2.

09-DEC-80 10:28:21

****

TAPE FILE: 27

ACCELERATION AMPLITUDE: 1000 rad/s^2

REFERENCE FREQUENCY: 15 Hz

REFERENCE SENSITIVITY: 5.529 uV/rad/s^2

****

FREQUENCY	SENSITIVITY	% DEVIATION	No. of READINGS
5.14	5.501	-0.6	3
6.91	5.434	-1.8	3
10.17	5.61	1.4	6
15.24	5.528	-0.1	9
30.23	5.581	0.9	3
70.46	5.864	6	6
100.34	5.958	7.7	6

****

Figure B-5B. Angular acceleration measurement results; sensitivity vs. frequency at an acceleration of 1000 rad/s^2.

09-DEC-80 10:31:07

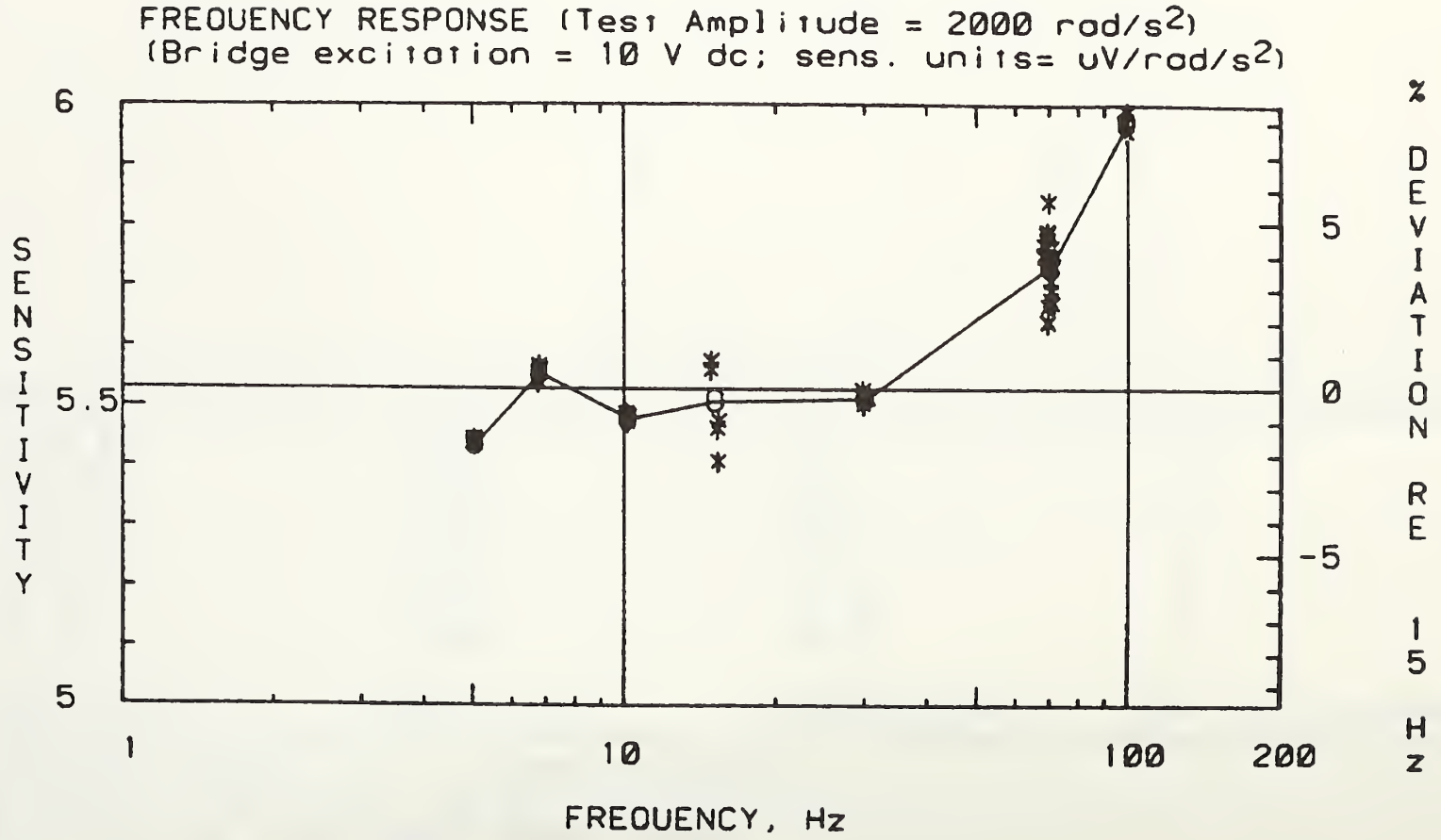

Figure B-6A. Angular acceleration measurement results; sensitivity vs. frequency at an acceleration of 2000 rad/s^2.

09-DEC-80 10:32:20

****

TAPE FILE: 28

ACCELERATION AMPLITUDE: 2000 rad/s^2

REFERENCE FREQUENCY: 15 Hz

REFERENCE SENSITIVITY: 5.529 uV/rad/s^2

****

FREQUENCY	SENSITIVITY	% DEVIATION	No. of READINGS
5.07	5.436	-1.7	3
6.82	5.553	0.4	3
10.22	5.479	-1	3
15.22	5.508	-0.4	6
30.18	5.513	-0.3	4
70.25	5.734	3.7	22
100.35	5.972	8	3

****

Figure B-6B. Angular acceleration measurement results; sensitivity vs. frequency at an acceleration of 2000 rad/s^2.

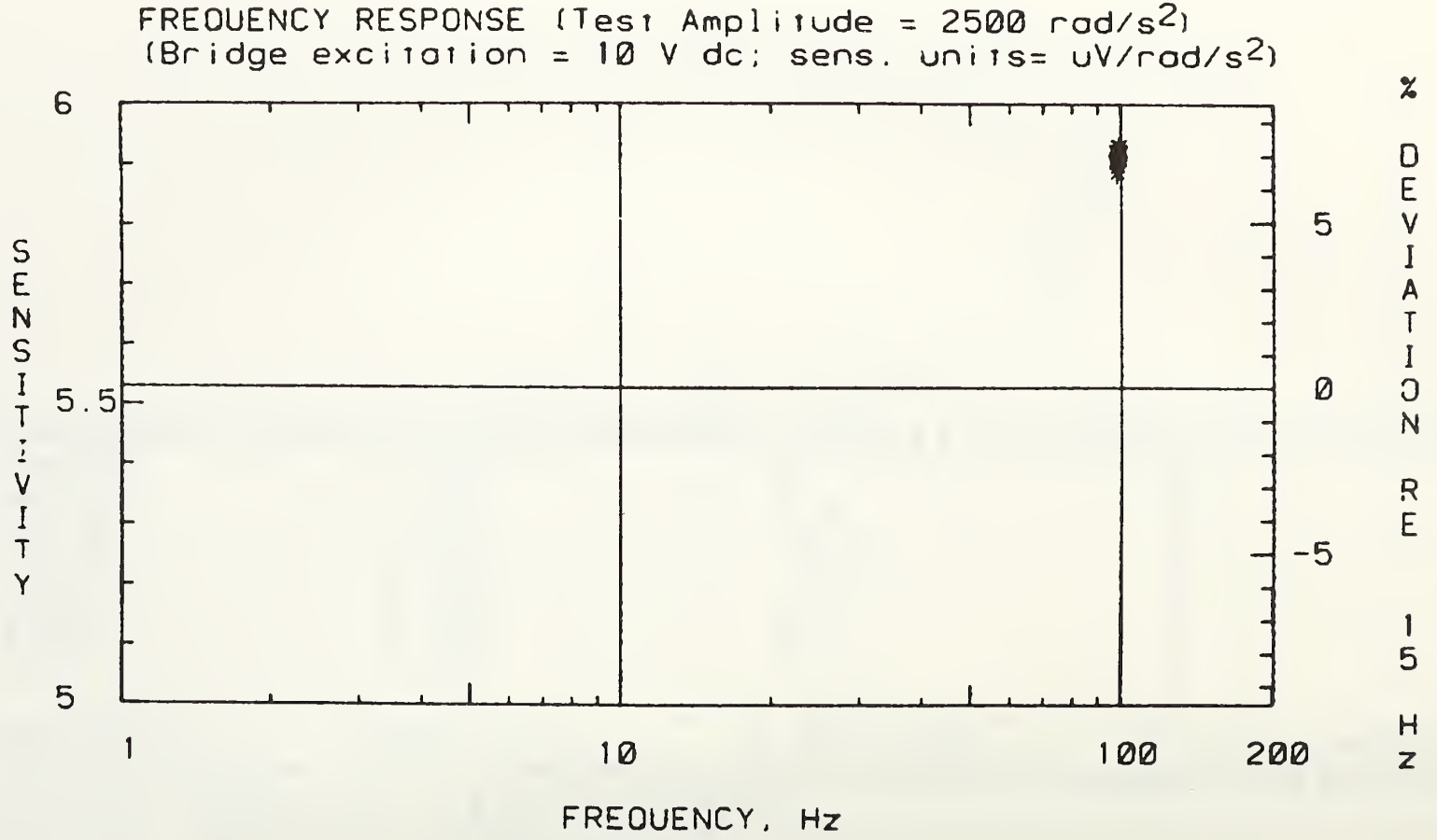

Figure B-7A. Angular acceleration measurement results; sensitivity vs. frequency at an acceleration of 2500 rad/s^2.

08-DEC-80 09:15:26

****

TAPE FILE: 32

ACCELERATION AMPLITUDE: 2500 rad/s^2

REFERENCE FREQUENCY: 15 Hz

REFERENCE SENSITIVITY: 5.529 uV/rad/s^2

****

FREQUENCY	SENSITIVITY	% DEVIATION	No. of READINGS
99.58	5.912	6.9	9

****

Figure B-7B. Angular acceleration measurement results; sensitivity vs. frequency at an acceleration of 2500 rad/s^2.

09-DEC-80 10:35:11

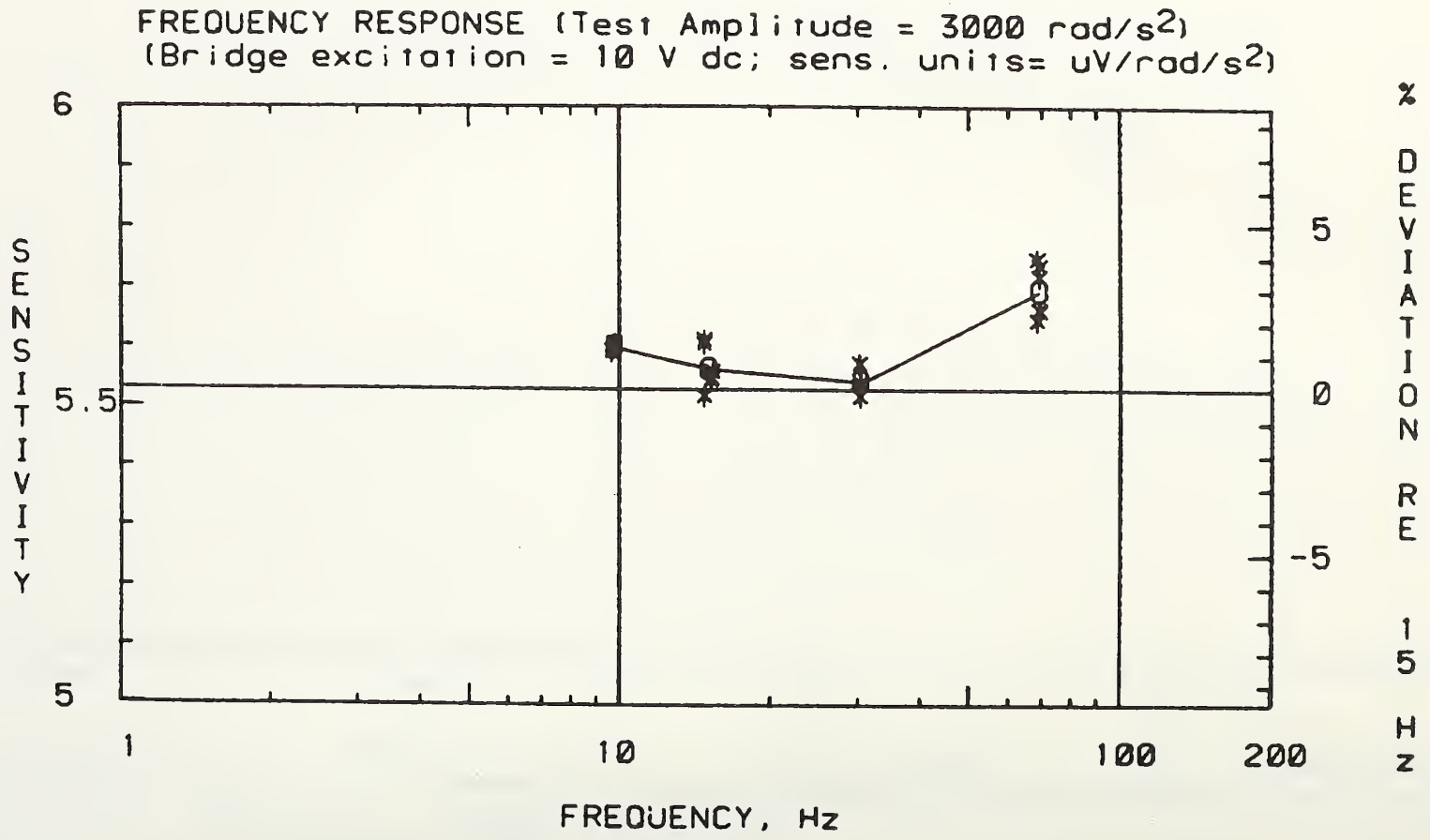

Figure B-8A. Angular acceleration measurement results; sensitivity vs. frequency at an acceleration of 3000 rad/s^2.

09-DEC-80 10:35:42

****

TAPE FILE: 29

ACCELERATION AMPLITUDE: 3000 rad/s^2

REFERENCE FREQUENCY: 15 Hz

REFERENCE SENSITIVITY: 5.529 uV/rad/s^2

****

FREQUENCY	SENSITIVITY	% DEVIATION	No. of READINGS
9.81	5.598	1.2	3
15.17	5.562	0.5	6
30.5	5.542	0.2	3
69.45	5.694	2.9	6

****

Figure B-8B. Angular acceleration measurement results; sensitivity vs. frequency at an acceleration of 3000 rad/s^2.

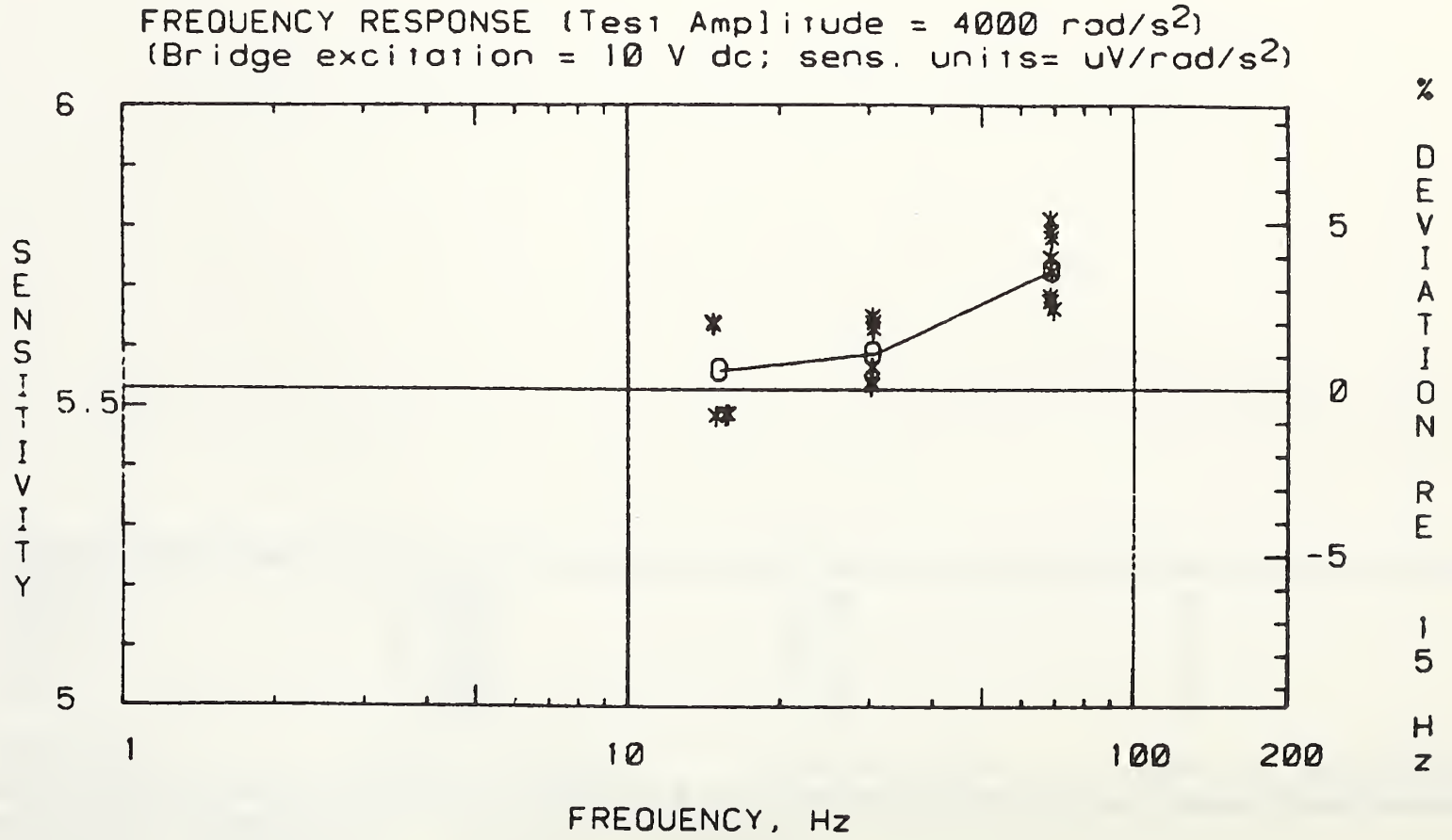

Figure B-9A. Angular acceleration measurement results; sensitivity vs. frequency at an acceleration of 4000 rad/s^2.

05-DEC-80 14:56:44

****

TAPE FILE: 30

ACCELERATION AMPLITUDE: 4000 rad/s^2

REFERENCE FREQUENCY: 15 Hz

REFERENCE SENSITIVITY: 5.529 uV/rad/s^2

****

FREQUENCY	SENSITIVITY	% DEVIATION	No. of READINGS
15.2	5.561	0.5	6
30.6	5.588	1	7
69.14	5.728	3.5	9

****

Figure B-9B. Angular acceleration measurement results; sensitivity vs. frequency at an acceleration of 4000 rad/s^2.

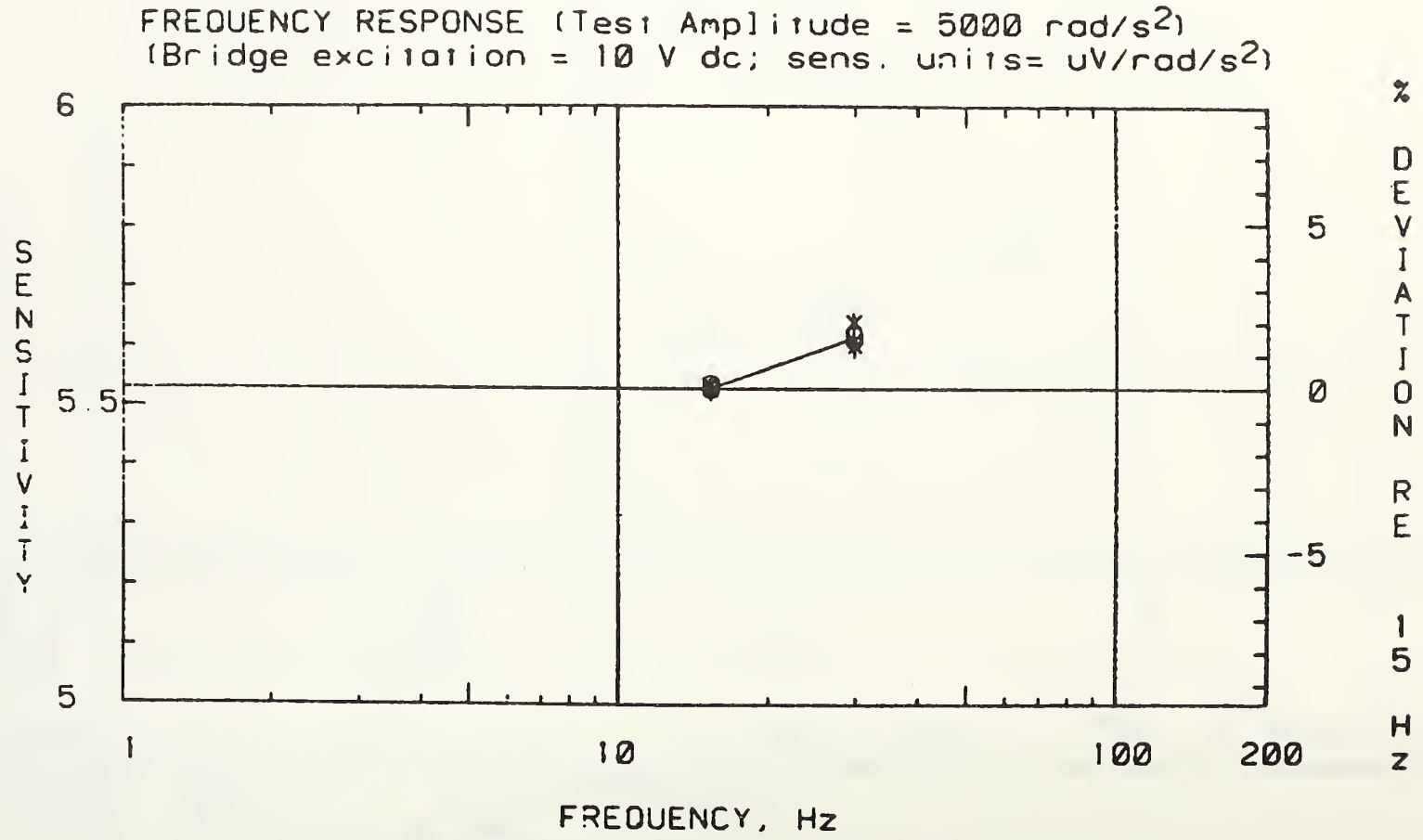

Figure B-10A. Angular acceleration measurement results; sensitivity vs. frequency at an acceleration of 5000 rad/s^2.

08-DEC-80 09:07:34

TAPE FILE: 31
ACCELERATION AMPLITUDE: 5000 rad/s^2
REFERENCE FREQUENCY: 15 Hz
REFERENCE SENSITIVITY: 5.529 uV/rad/s^2

FREQUENCY	SENSITIVITY	% DEVIATION	No. of READINGS
15.42	5.531	0	3
29.99	5.615	1.5	3

Figure B-10B. Angular acceleration measurement results; sensitivity vs. frequency at an acceleration of 5000 rad/s^2.

NBS-114A (REV. 2-8C)

U.S. DEPT. OF COMM. BIBLIOGRAPHIC DATA SHEET (See instructions)	1. PUBLICATION OR REPORT NO. NBSIR 81-2337	2. Performing Organ. Report No.	3. Publication Date August 1981

4. TITLE AND SUBTITLE

Measurement and Evaluation Methods for an Angular Accelerometer

5. AUTHOR(S)

John D. Ramboz

6. PERFORMING ORGANIZATION (If joint or other than NBS, see instructions)

NATIONAL BUREAU OF STANDARDS
DEPARTMENT OF COMMERCE
WASHINGTON, D.C. 20234

7. Contract/Grant No.

DOT-HS-9-02193IA

8. Type of Report & Period Covered

Final Report
8/1/80 - 12/30/80

9. SPONSORING ORGANIZATION NAME AND COMPLETE ADDRESS (Street, City, State, ZIP)

Department of Transportation
National Highway Traffic Safety Administration
400 Seventh St., S.W.
Washington, D.C. 20590

10. SUPPLEMENTARY NOTES

☐ Document describes a computer program; SF-185, FIPS Software Summary, is attached.

11. ABSTRACT (A 200-word or less factual summary of most significant information. If document includes a significant bibliography or literature survey, mention it here)

A transducer which measures angular acceleration along one axis was investigated to assess three of its performance characteristics, viz., sensitivity factor, amplitude linearity, and response to linear (non-angular) input accelerations. Accelerometer specifications and response theory are presented. Test philosophy and methodology are discussed along with measurement results. Tests were conducted over a frequency range from 1.5 to 100 Hz and an acceleration range from 64 to 5000 rad/s^2. Generally, the performance observed was in agreement with the manufacturer's preliminary specifications.

12. KEY WORDS (Six to twelve entries; alphabetical order; capitalize only proper names; and separate key words by semicolons)

Angular acceleration; angular accelerometer; calibration; instrumentation; measurement; shock and vibration.

13. AVAILABILITY

☒ Unlimited
☐ For Official Distribution. Do Not Release to NTIS
☐ Order From Superintendent of Documents, U.S. Government Printing Office, Washington, D.C. 20402.
☒ Order From National Technical Information Service (NTIS), Springfield, VA. 22161

14. NO. OF PRINTED PAGES

78

15. Price

$9.50